International Telecommunication Union

ITU-R
Radiocommunication Sector of ITU

Recommendation ITU-R P.681-10
(12/2017)

Propagation data required for the design of Earth-space land mobile telecommunication systems

P Series

Radiowave propagation

International Telecommunication Union

Foreword

The role of the Radiocommunication Sector is to ensure the rational, equitable, efficient and economical use of the radio-frequency spectrum by all radiocommunication services, including satellite services, and carry out studies without limit of frequency range on the basis of which Recommendations are adopted.

The regulatory and policy functions of the Radiocommunication Sector are performed by World and Regional Radiocommunication Conferences and Radiocommunication Assemblies supported by Study Groups.

Policy on Intellectual Property Right (IPR)

ITU-R policy on IPR is described in the Common Patent Policy for ITU-T/ITU-R/ISO/IEC referenced in Annex 1 of Resolution ITU-R 1. Forms to be used for the submission of patent statements and licensing declarations by patent holders are available from http://www.itu.int/ITU-R/go/patents/en where the Guidelines for Implementation of the Common Patent Policy for ITU-T/ITU-R/ISO/IEC and the ITU-R patent information database can also be found.

<div style="border:1px solid">

Series of ITU-R Recommendations

(Also available online at http://www.itu.int/publ/R-REC/en)

Series	Title
BO	Satellite delivery
BR	Recording for production, archival and play-out; film for television
BS	Broadcasting service (sound)
BT	Broadcasting service (television)
F	Fixed service
M	Mobile, radiodetermination, amateur and related satellite services
P	**Radiowave propagation**
RA	Radio astronomy
RS	Remote sensing systems
S	Fixed-satellite service
SA	Space applications and meteorology
SF	Frequency sharing and coordination between fixed-satellite and fixed service systems
SM	Spectrum management
SNG	Satellite news gathering
TF	Time signals and frequency standards emissions
V	Vocabulary and related subjects

</div>

Note: *This ITU-R Recommendation was approved in English under the procedure detailed in Resolution ITU-R 1.*

Electronic Publication
Geneva, 2017

© ITU 2017

RECOMMENDATION ITU-R P.681-10*

Propagation data required for the design of Earth-space land mobile telecommunication systems

(Question ITU-R 207/3)

(1990-1994-1995-1997-1999-2001-2003-2009-2015-2016-2017)

Scope

This Recommendation predicts the various propagation parameters needed in planning the Earth-space land mobile-satellite service (LMSS).

The ITU Radiocommunication Assembly,

considering

a) that for the proper planning of Earth-space land mobile systems it is necessary to have appropriate propagation data and prediction methods;

b) that the methods of Recommendation ITU-R P.618 are recommended for the planning of Earth-space telecommunication systems;

c) that further development of prediction methods for specific application to land mobile-satellite systems is required to give adequate accuracy in all regions of the world and for all operational conditions;

d) that, however, methods are available which yield sufficient accuracy for many applications,

recommends

that the methods contained in Annex 1 be adopted for use in the planning of Earth-space land mobile telecommunication systems, in addition to the methods recommended in Recommendation ITU-R P.618.

Annex 1

1 Introduction

Propagation effects in the land mobile-satellite service (LMSS) differ from those of the fixed-satellite service (FSS) primarily because of the greater importance of terrain effects. In the FSS it is generally possible to discriminate against multipath, shadowing and blockage through the use of highly directive antennas placed at unobstructed sites. Therefore, in general, the LMSS offers smaller link availability percentages than the FSS. The prime availability range of interest to system designers is usually from 80% to 99%.

---

* This Recommendation should be brought to the attention of Radiocommunication Study Group 4.

This Annex deals with data and models specifically needed for predicting propagation impairments in LMSS links, which include tropospheric effects, ionospheric effects, multipath, blockage and shadowing. It is based on measurements ranging from 870 MHz in the UHF band up to 20 GHz.

2   Tropospheric effects

2.1   Attenuation

Signal losses in the troposphere are caused by atmospheric gases, rain, fog and clouds. Except at low elevation angles, tropospheric attenuation is negligible at frequencies below about 1 GHz, and is generally small at frequencies up to about 10 GHz. Above 10 GHz, the attenuation can be large for significant percentages of the time on many paths. Prediction methods are available for estimating gaseous absorption (Recommendation ITU-R P.676) and rain attenuation (Recommendation ITU-R P.618). Fog and cloud attenuation is usually negligible for frequencies up to 10 GHz.

2.2   Scintillation

Irregular variations in received signal level and in angle of arrival are caused by both tropospheric turbulence and atmospheric multipath. The magnitudes of these effects increase with increasing frequency and decreasing path elevation angle, except that angle-of-arrival fluctuations caused by turbulence are independent of frequency. Antenna beamwidth also affects the magnitude of these scintillations. These effects are observed to be at a maximum in the summer season. A prediction method is given in Recommendation ITU-R P.618.

3   Ionospheric effects

Ionospheric effects on Earth-to-space paths are addressed in Recommendation ITU-R P.531. Values of ionospheric effects for frequencies in the range of 0.1 to 10 GHz are given in Tables 1 and 2 of Recommendation ITU-R P.680.

4   Shadowing

4.1   Roadside tree-shadowing model

Cumulative fade distribution measurements at 870 MHz, 1.6 GHz and 20 GHz have been used to develop the extended empirical roadside shadowing model. The extent of trees along the roadside is represented by the percentage of optical shadowing caused by roadside trees at a path elevation angle of 45° in the direction of the signal source. The model is valid when this percentage is in the range of 55% to 75%.

4.1.1   Calculation of fading due to shadowing by roadside trees

The following procedure provides estimates of roadside shadowing for frequencies between 800 MHz and 20 GHz, path elevation angles from 7° up to 60°, and percentages of distance travelled from 1% to 80%. The empirical model corresponds to an average propagation condition with the vehicle driving in lanes on both sides of the roadway (lanes close to and far from the roadside trees are included). The predicted fade distributions apply for highways and rural roads where the overall aspect of the propagation path is, for the most part, orthogonal to the lines of roadside trees and utility poles and it is assumed that the dominant cause of LMSS signal fading is tree canopy shadowing (see Recommendation ITU-R P.833).

Parameters required are the following:

f: frequency (GHz)

θ: path elevation angle to the satellite (degrees)

p: percentage of distance travelled over which fade is exceeded.

Step 1: Calculate the fade distribution at 1.5 GHz, valid for percentages of distance travelled of $20\% \geq p \geq 1\%$, at the desired path elevation angle, $60° \geq \theta \geq 20°$:

$$A_L(p,\theta) = -M(\theta) \ln (p) + N(\theta) \tag{1}$$

where:

$$M(\theta) = 3.44 + 0.0975\,\theta - 0.002\,\theta^2 \tag{2}$$

$$N(\theta) = -0.443\,\theta + 34.76 \tag{3}$$

Step 2: Convert the fade distribution at 1.5 GHz, valid for $20\% \geq p \geq 1\%$, to the desired frequency, f (GHz), where 0.8 GHz $\leq f \leq 20$ GHz:

$$A_{20}(p, \theta, f) = A_L(p, \theta) \exp \left\{ 1.5 \left[\frac{1}{\sqrt{f_{1.5}}} - \frac{1}{\sqrt{f}} \right] \right\} \tag{4}$$

Step 3: Calculate the fade distribution for percentages of distance travelled $80\% \geq p > 20\%$ for the frequency range 0.85 GHz $\leq f \leq 20$ GHz as:

$$A(p, \theta, f) = A_{20}(20\%, \theta, f)\, \frac{1}{\ln 4} \ln\left(\frac{80}{p}\right) \qquad \text{for} \quad 80\% \geq p > 20\% \tag{5}$$

$$= A_{20}(p, \theta, f) \qquad \text{for} \quad 20\% \geq p > 1\%$$

Step 4: For path elevation angles in the range $20° > \theta \geq 7°$, the fade distribution is assumed to have the same value as at $\theta = 20°$.

Figure 1 shows fades exceeded at 1.5 GHz versus elevation angles between 10° and 60° for a family of equal percentages between 1% and 50%.

4.1.1.1 Extension to elevation angles > 60°

The roadside shadowing model at frequencies of 1.6 GHz and 2.6 GHz can be extended to elevation angles above 60° with the following procedure:

– apply equations (1) to (5) at an elevation angle of 60° at the above frequencies;

– linearly interpolate between the value calculated for an angle of 60° and the fade values for an elevation angle of 80° provided in Table 1;

– linearly interpolate between the values in Table 1 and a value of zero at 90°.

FIGURE 1

Fading at 1.5 GHz due to roadside shadowing versus path elevation angle
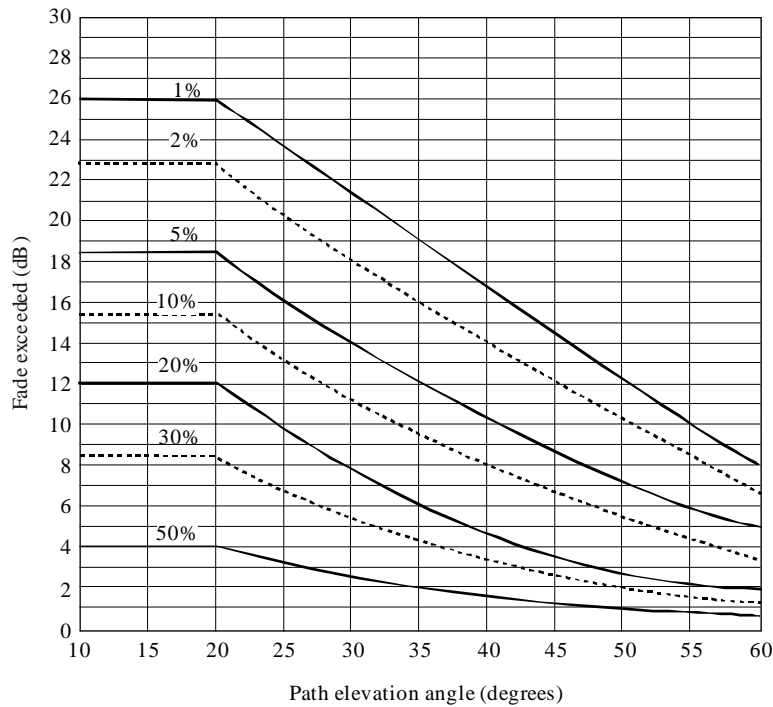
P.0681-01

TABLE 1

Fades exceeded (dB) at 80° elevation

p (%)	Tree-shadowed	
	1.6 GHz	2.6 GHz
1	4.1	9.0
5	2.0	5.2
10	1.5	3.8
15	1.4	3.2
20	1.3	2.8
30	1.2	2.5

4.1.1.2   Application of roadside shadowing model to non-geostationary (non-GSO) and mobile-satellite systems

The prediction method above was derived for, and is applied to, LMSS geometries where the elevation angle remains constant. For non-GSO systems, where the elevation angle is varying, the link availability can be calculated in the following way:

a)   calculate the percentage of time for each elevation angle (or elevation angle range) under which the terminal will see the spacecraft;

b)   for a given propagation margin (ordinate of Fig. 1), find the percentage of unavailability for each elevation angle;

c)   for each elevation angle, multiply the results of step a) and b) and divide by 100, giving the percentage of unavailability of the system at this elevation;

d)   add up all unavailability values obtained in step c) to arrive at the total system unavailability.

If the antenna used at the mobile terminal does not have an isotropic pattern, the antenna gain at each elevation angle has to be subtracted from the fade margin in step b) above.

In the case of multi-visibility satellite constellations employing satellite path diversity (i.e. switching to the least impaired path), an approximate calculation can be made assuming that the spacecraft with the highest elevation angle is being used.

4.1.2   Fade duration distribution model

Optimal design of LMSS receivers depends on knowledge of the statistics associated with fade durations, which can be represented in units of travelled distance (m) or (s). Fade duration measurements have given rise to the following empirical model which is valid for distance fade duration $dd \geq 0.02$ m.

$$P(FD > dd \mid A > A_q) = \frac{1}{2}\left(1 - \mathrm{erf}\left[\frac{\ln(dd) - \ln(\alpha)}{\sqrt{2}\,\sigma}\right]\right) \tag{6}$$

where $P(FD > dd \mid A > A_q)$ represents the probability that the distance fade duration, FD, exceeds the distance, dd (m), under the condition that the attenuation, A, exceeds A_q. The designation "erf" represents the error function, σ is the standard deviation of $\ln(dd)$, and $\ln(\alpha)$ is the mean value of $\ln(dd)$. The left-hand side of equation (6) was estimated by computing the percentage number of "duration events" that exceed dd relative to the total number of events for which $A > A_q$ in data obtained from measurements in the United States of America and Australia. The best fit regression values obtained from these measurements are $\alpha = 0.22$ and $\sigma = 1.215$.

Figure 2 contains a plot of P, expressed as a percentage, p, versus dd for a 5 dB threshold.

The model given by equation (6) is based on measurements at an elevation angle of 51° and is applicable for moderate to severe shadowing (percentage of optical shadowing between 55% and 90%). Tests at 30° and 60° have demonstrated a moderate dependence on elevation angle: the smaller the elevation angle, the larger is the fade duration for a fixed percentage. For example, the 30° fade duration showed approximately twice that for the 60° fade duration at the same percentage level.

4.1.3   Non-fade duration distribution model

A non-fade duration event of distance duration, dd, is defined as the distance over which the fade levels are smaller than a specified fade threshold. The non-fade duration model is given by:

$$p(NFD > dd \mid A < A_q) = \beta\,(dd)^{-\gamma} \tag{7}$$

where $p(NFD > dd \mid A < A_q)$ is the percentage probability that a continuous non-fade distance, NFD, exceeds the distance, dd, given that the fade is smaller than the threshold, A_q. Table 2 contains the values of β and γ for roads that exhibit moderate and extreme shadowing i.e. the percentage of optical shadowing of between 55% and 75% and between 75% and 90% respectively. A 5 dB fade threshold is used for A_q.

FIGURE 2

**Best fit cumulative fade distribution for roadside tree
shadowing with a 5 dB threshold**
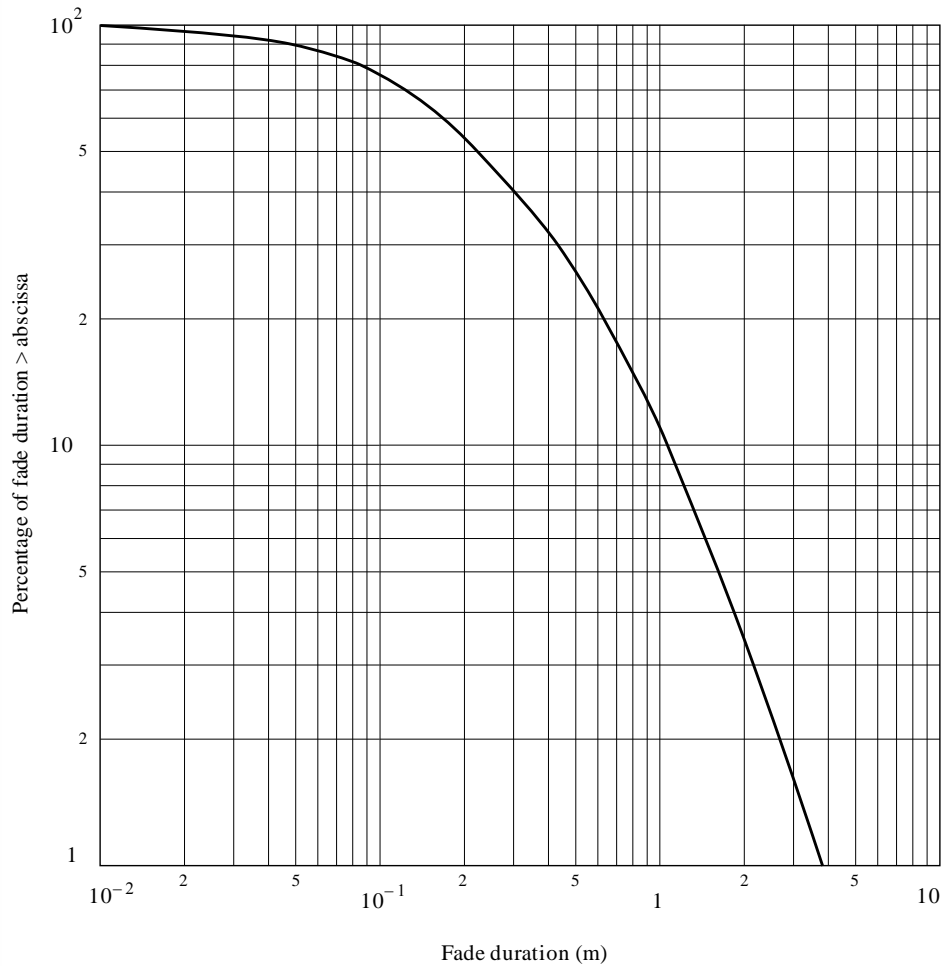
Fade duration (m)

P.0681-02

TABLE 2

**Non-fade duration regression values for a 5 dB fade threshold
at a path elevation angle of 51°**

Shadowing level	β	γ
Moderate	20.54	0.58
Extreme	11.71	0.8371

4.2   Roadside building-shadowing model

Shadowing by roadside buildings in an urban area can be modelled by assuming a Rayleigh distribution of building heights. Figure 3 shows the geometry.

FIGURE 3

Geometry of roadside building shadowing model
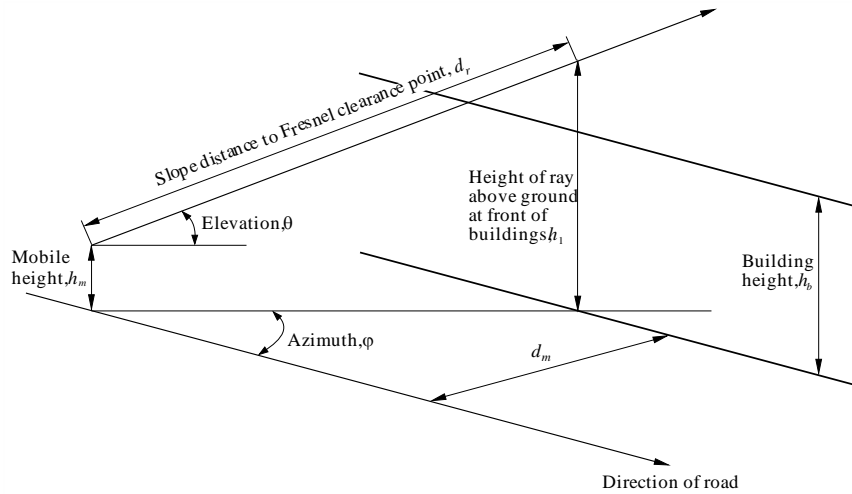
P.0681-03

The percentage probability of blockage due to the buildings is given by:

$$p = 100 \exp\left[-(h_1 - h_2)^2 / 2h_b^2\right] \qquad \text{for} \quad h_1 > h_2 \qquad (8)$$

where:

h_1 : height of the ray above ground at the building frontage, given by:
$$h_1 = h_m + (d_m \tan \theta / \sin \varphi) \qquad (8a)$$

h_2 : Fresnel clearance distance required above buildings, given by:
$$h_2 = C_f \ (\lambda \ d_r)^{0.5} \qquad (8b)$$

h_b : the most common (modal) building height

h_m : height of mobile above ground

θ : elevation angle of the ray to the satellite above horizontal

φ : azimuth angle of the ray relative to street direction

d_m : distance of the mobile from the front of the buildings

d_r : slope distance from the mobile to the position along the ray vertically above building front, given by:
$$d_r = d_m / (\sin \varphi \cdot \cos \theta) \qquad (8c)$$

C_f : required clearance as a fraction of the first Fresnel zone

λ : wavelength

and where h_1, h_2, h_b, h_m, d_m, d_r and λ are in self-consistent units, and $h_1 > h_2$.

Note that equations (8a), (8b) and (8c) are valid for $0 < \theta < 90°$ and for $0 < \varphi < 180°$. The actual limiting values should not be used.

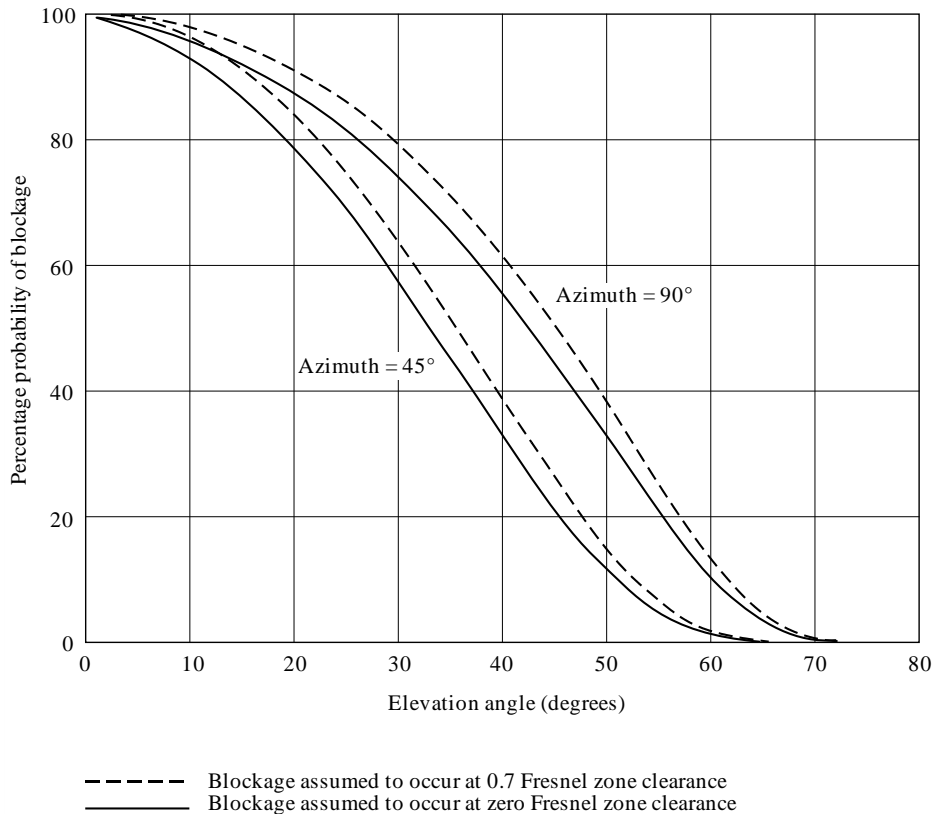Figure 4 shows examples of roadside building shadowing computed using the above expressions for:

$h_b = 15$ m

$h_m = 1.5$ m

$d_m = 17.5$ m

Frequency = 1.6 GHz.

FIGURE 4

Examples of roadside building shadowing
(see text for parameter values)

Azimuth = 90°

Azimuth = 45°

- - - - -   Blockage assumed to occur at 0.7 Fresnel zone clearance
———————   Blockage assumed to occur at zero Fresnel zone clearance

P.0681-04

In Fig. 4 the dashed lines apply when blocking is considered to exist if the ray has a clearance less than 0.7 of the first Fresnel Zone vertically above the building front. The solid lines apply when blocking is considered to exist only when there is no line-of-sight.

Although the model indicates no blockage at the highest path elevation angles, users should be aware that occasional shadowing and blockage can occur from overpasses, overhanging standards, branches, etc.

4.3   Special consideration of hand-held terminals (user blockage)

When using hand-held communication terminals, the operator's head or body in the near-field of the antenna causes the antenna pattern to change. For the case of non-low Earth orbit (non-LEO) satellite systems (GSO, high Earth orbit (HEO), ICO), the user of the hand-held terminal is expected to be cooperative, i.e. to position himself in such a way as to avoid blockage from both the head (or body) and the environment. For LEO systems this assumption cannot be made. The influence of the head (or body) can be evaluated by including the modified antenna pattern (which has to be measured) in the link availability calculation as presented in § 4.1.1.2. Assuming that the azimuth angles under which the satellite is seen are evenly distributed, an azimuth-averaged elevation pattern can be applied. The small movements of the head or hand which lead to small variations in apparent elevation angle can also be averaged.

Relating to this effect, a field experiment was performed in Japan. Figure 5a shows the geometry of a human head and an antenna in the experiment. The satellite elevation angle is 32° and the satellite signal frequency is 1.5 GHz. The antenna gain is 1 dBi and the length is 10 cm. Figure 5b shows the variation of relative signal level versus azimuth angle φ in Fig. 5a. It can be seen from Fig. 5b that the maximum reduction in signal level due to user blockage is about 6 dB when the equipment is in the shadow region of the human head.

The results presented in Fig. 5b are intended to be illustrative only, since the data correspond to a single elevation angle and antenna pattern, and no account is taken of potential specular reflection effects, which may play a significant role in a hand-held environment where little directivity is provided.

Propagation data related to signal entry loss for reception within buildings and vehicles, of particular interest for hand-held terminals, may be found in Recommendation ITU-R P.679.

4.4 Modelling building blockage effects using street masking functions (MKF)

Building blockage effects can also be quantified using street MKFs indicating the azimuths and elevations for which a link can or cannot be completed. Functions of this type have often been obtained by means of photogrametric studies or ray-tracing. The MKF concept can be applied to simplified scenarios to produce a limited number of MKFs and hence, making it possible to produce fast, approximate assessments of the combined availability in different multi-satellite configurations.

A given urban area could be described, as a first approximation, by an average masking angle (MKA) (degrees).

The MKA is defined as the satellite elevation for grazing incidence with building tops when the link is perpendicular to the street or in mathematical terms:

$$MKA = \arctan\left(\frac{h}{w/2}\right) \qquad \text{degrees} \qquad (9)$$

where:

h : average building height

w : average street width.

Further, an urban scenario with a given MKA can be assumed to be made up of a combination of a small number of typical configurations (basic/constitutive scenarios), namely, street canyons (scy), street crossings (scr), T-junctions (T-j) and single walls (sw), each with a given occurrence probability (see Fig. 5). Similarly a path-mixture vector, $\vec{M}$, could be defined, stating, for a given built-up area, the probabilities of encountering each of the constitutive scenarios $\vec{M}$ (w_{scy}, w_{scr}, w_{T-j}, w_{sw}), with $\sum w_i = 1$. Input data to this model, i.e., MKA, can be obtained by observation of the environment or from city maps.

FIGURE 5

Basic/constitutive scenarios describing a given urban area
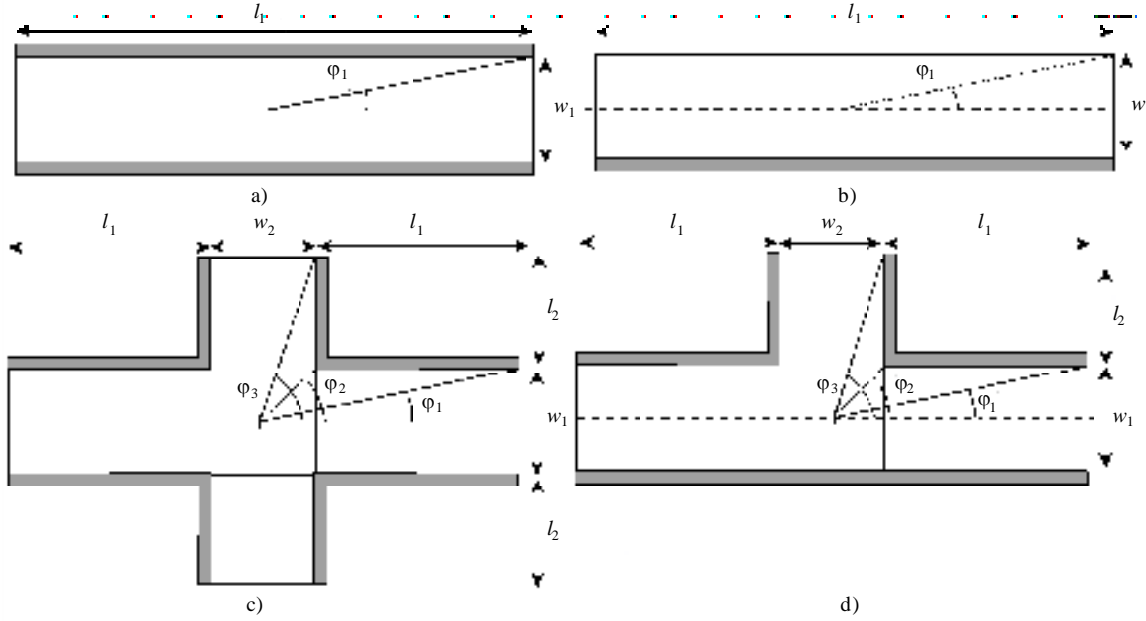
P.0681-05

If availability probabilities are worked out for those four constitutive scenarios, the overall availability could be roughly estimated as the weighted sum of the availabilities in each scenario:

$$a_T = w_{scy}\, a_{scy} + w_{scr}\, a_{scr} + w_{T\text{-}j}\, a_{T\text{-}j} + w_{sw}\, a_{sw} \tag{10}$$

The MKFs for these four basic scenarios have been constructed by means of simple geometry assuming the user is in the middle of the scene (see Fig. 5). Considering a simple on-off, or line-of-sight − non-line-of-sight, propagation model (as in § 4.2 for the zero Fresnel zone clearance case), the MKFs of the four constitutive urban scenarios are presented in Fig. 6 where the ordinates indicate elevation angles and the abscissas azimuths or, rather, street orientations, ξ, with respect to the link. The top half-plane indicates positive azimuths and the bottom half-plane corresponds to negative azimuths. A MKF indicates the regions in the celestial hemisphere where a link can be completed (non-shaded) or not (shaded areas). The contours delimiting the "forbidden" zones in the MKFs are defined by segments and points. The most relevant ones are illustrated in Fig. 6 and given by the following equations:

$$S_A: \quad \theta = \tan^{-1}\!\left(h\,/\,\sqrt{\left(\frac{w}{2}\right)^2\!\left(\frac{1}{\tan^2\varphi}+1\right)}\,\right) \tag{11a}$$

$$P_A: \quad \left(\varphi_A = 90°\,;\, \theta_A = \tan^{-1}\!\left(\frac{h}{w/2}\right) \right) \tag{11b}$$

$$S_{B_1}: \quad \theta = \tan^{-1}\!\left(h\,/\,\sqrt{\left(\frac{w_1}{2}\right)^2\!\left(\frac{1}{\tan^2\varphi}+1\right)}\,\right) \tag{11c}$$

$$S_{B_2}: \quad \theta = \tan^{-1}\left(h\,/\,\sqrt{\left(\frac{w_1}{2}\right)^2\left(\frac{1}{\tan^2(90° - \varphi)} + 1\right)}\,\right) \tag{11d}$$

$$P_B: \quad \left(\varphi_B = \tan^{-1}\left(\frac{w_1}{w_2}\right); \quad \theta_2 = \tan^{-1}\left(h\,/\,\sqrt{\left(\frac{w_1}{2}\right)^2\left(\frac{1}{\tan^2\varphi_B} + 1\right)}\,\right) \right) \tag{11e}$$

FIGURE 6

**MKFs of a) a street canyon, b) a single wall,
c) a street crossing and d) a T-junction**

$h = 20$
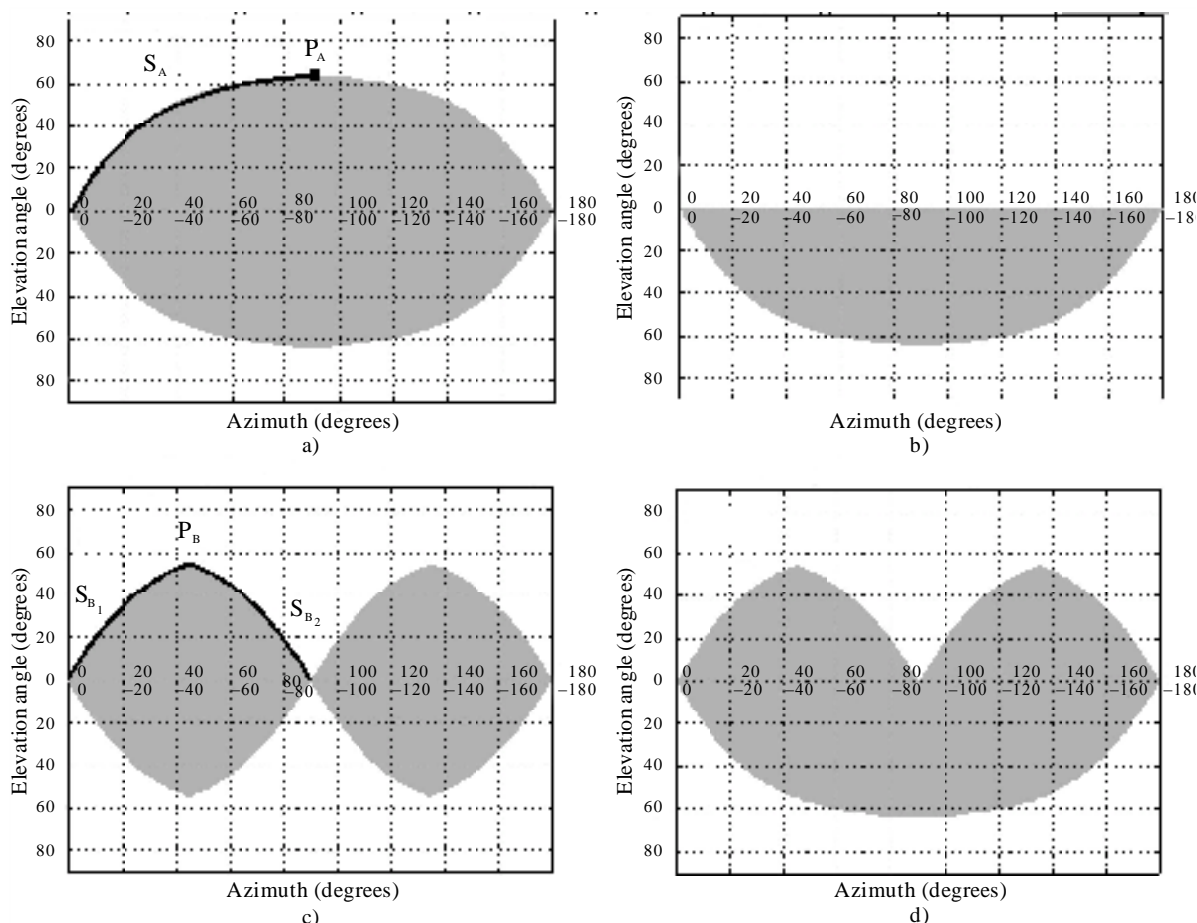
$w_1 = 20$

$w_2 = 20$

$MKA \approx 63°$

P.0681-06

The availability for a particular basic scenario and a given geostationary (GSO) satellite can be computed by considering all possible street orientations, ξ, with respect to the user-satellite link. In Fig. 7 the position of a GSO satellite with respect to a T-junction is indicated. For the case illustrated in the Figure all possible orientations can be described by sweeping through all points in line A-B corresponding to a constant elevation angle and all possible street orientations. The availability is the fraction of the straight line A-B in the non-shaded part of the MKF. Similarly, a non-GSO orbit

trajectory can be drawn on an MKF. The overall availability can be computed in this case by considering all possible street orientations with respect to all possible user-satellite link directions.

FIGURE 7

Calculation of the availability for a T-junction and a GSO satellite

$h = 20$

$w_1 = 20$

$w_2 = 20$

$MKA \approx 63°$
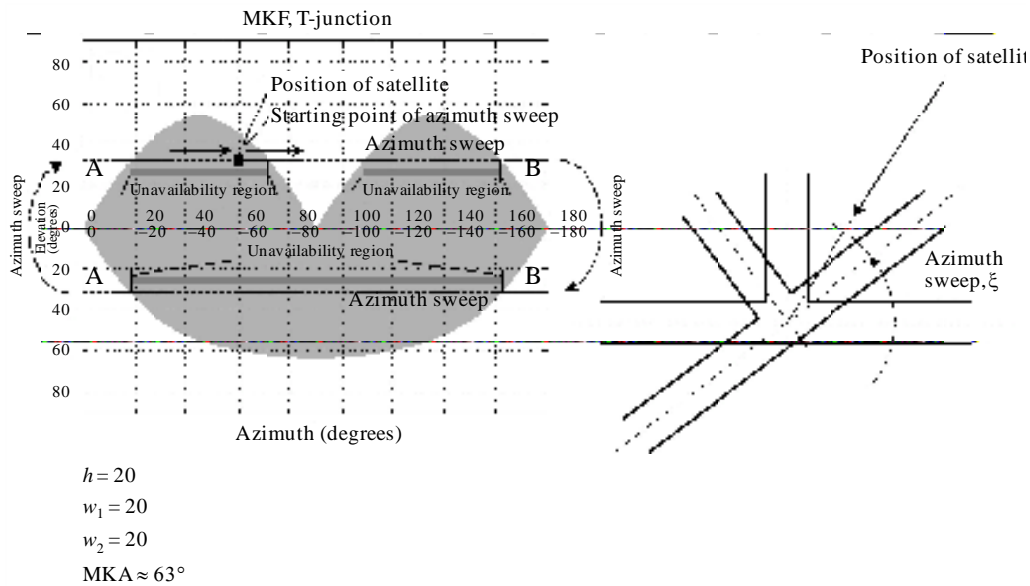
P.0681-07

5 Multipath models for clear line-of-sight conditions

In many cases the mobile terminal has a clear line-of-sight (negligible shadowing) to the mobile satellite. Degradation to the signal can still occur under these circumstances, due to terrain-induced multipath. The mobile terminal receives a phasor summation of the direct line-of-sight signal and several multipath signals. These multipath signals may add constructively or destructively to result in signal enhancement or fade. The multipath signal characteristics depend on the scattering cross-sections of the multipath reflectors, their number, the distances to the receiving antenna, the field polarizations, and receiving antenna gain pattern.

The multipath degradation models introduced in the following sections are based on measurements made using an antenna with the following characteristics:

– omnidirectional in azimuth;

– gain variation between 15° and 75° elevation less than 3 dB;

– below the horizon (negative elevation angles) the antenna gain was reduced by at least 10 dB.

FIGURE 8

a) Geometry of a human head and an antenna;

b) Fading at 1.5 GHz due to roadside shadowing versus path elevation angle

Satellite signal

Human head

Antenna

φ

5 cm

Human head

Antenna (quadrifilar helix)

d

32°

177 cm

Ground

Top view

Side view

Satellite

Satellite

Average received level in line-of-sight condition

Azimuth angle φ (degrees)

Relative signal level (dB)

d = −17 cm

d = −9 cm   Elevation angle = 32°

d = +3 cm

P0681-08
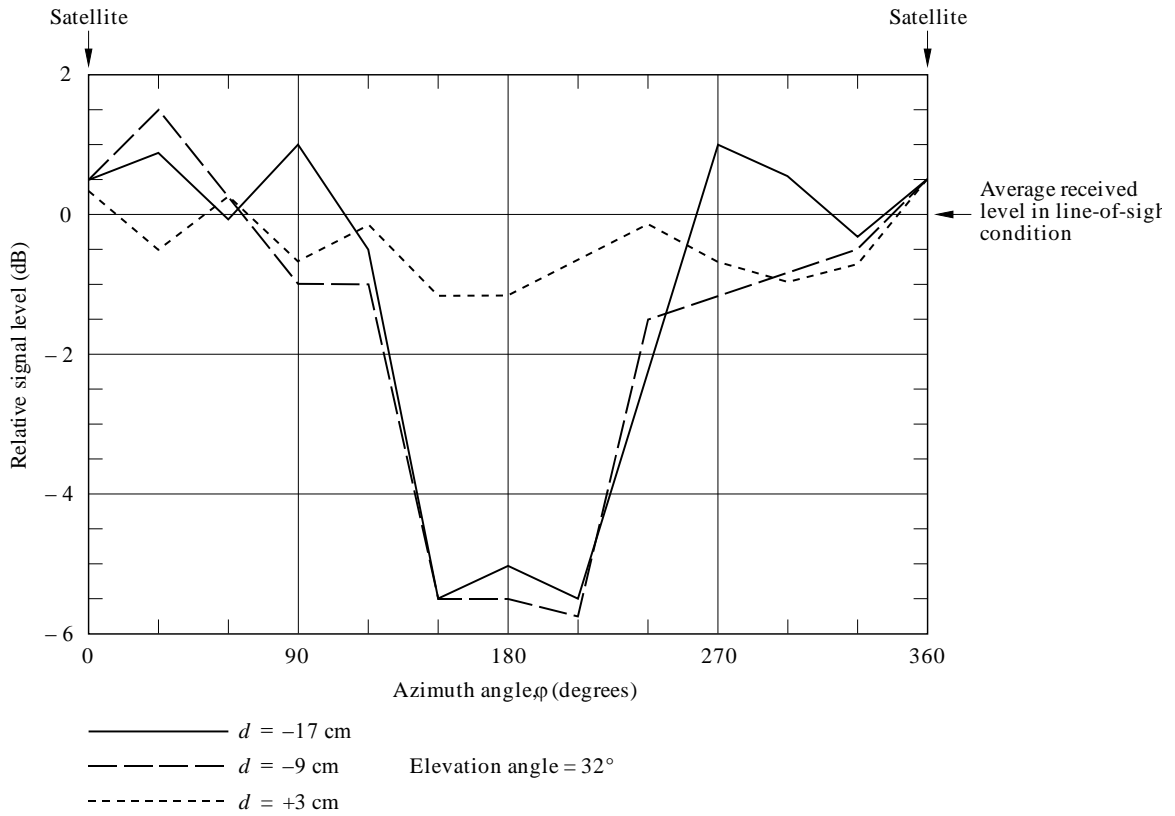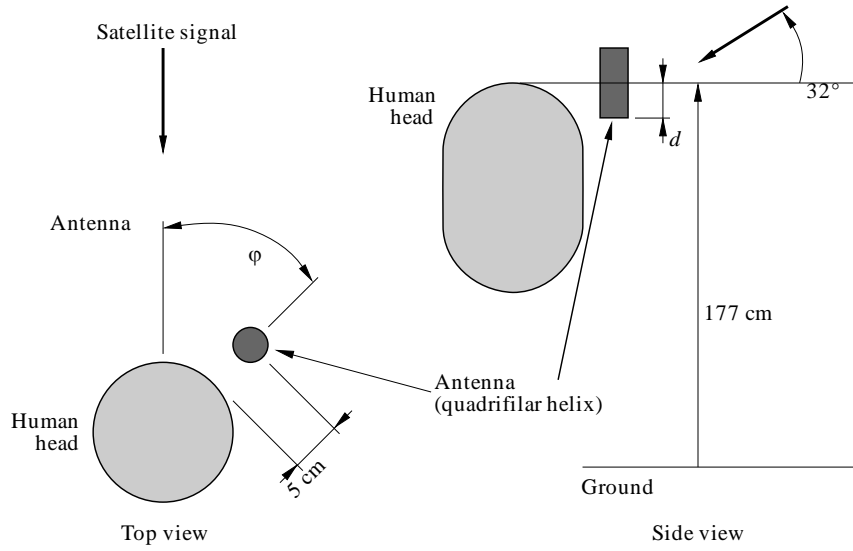
5.1   Multipath in a mountain environment

The distribution of fade depths due to multipath in mountainous terrain is modelled by:

$$p = a \, A^{-b} \tag{12}$$

for:

$$1\% < p < 10\%$$

where:

        p :   percentage of distance over which the fade is exceeded

        A :   fade exceeded (dB).

The curve fit parameters, a and b, are shown in Table 3 for 1.5 GHz and 870 MHz. Note that the above model is valid when the effect of shadowing is negligible.

TABLE 3

**Parameters for best fit cumulative fade distribution
for multipath in mountainous terrain**

Frequency (GHz)	Elevation = 30°			Elevation = 45°		
	a	b	Range (dB)	a	b	Range (dB)
0.87	34.52	1.855	2-7	31.64	2.464	2-4
1.5	33.19	1.710	2-8	39.95	2.321	2-5

Figure 9 contains curves of the cumulative fade distributions for path elevation angles of 30° and 45° at 1.5 GHz and 870 MHz.

5.2   Multipath in a roadside tree environment

Experiments conducted along tree-lined roads in the United States of America have shown that multipath fading is relatively insensitive to path elevation over the range of 30° to 60°. The measured data have given rise to the following model:

$$p = u \exp(-vA) \tag{13}$$

for:

$$1\% < p < 50\%$$

where:

        p :   percentage of distance over which the fade is exceeded

        A :   fade exceeded (dB).

Note that the above model assumes negligible shadowing. The curve fit parameters, u and v, are shown in Table 4.

FIGURE 9

Best fit cumulative fade distributions for multipath fading in mountainous terrain
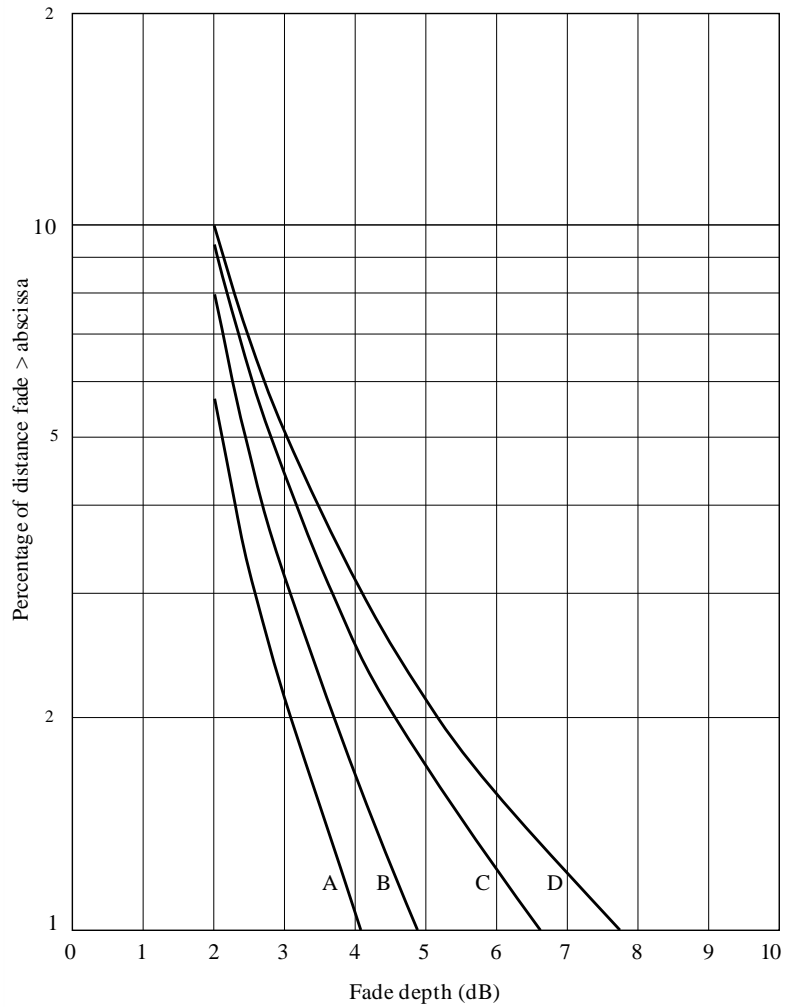
Curves A: 870 MHz, 45°
B: 1.5 GHz, 45°
C: 870 MHz, 30°
D: 1.5 GHz, 30°

P.0681-09

TABLE 4

**Parameters for best exponential fit cumulative fade distributions
for multipath for tree-lined roads**

Frequency (GHz)	u	v	Fade range (dB)
0.870	125.6	1.116	1-4.5
1.5	127.7	0.8573	1-6

Figure 10 contains curves of the cumulative fade distributions for 1.5 GHz and 870 MHz. Enhanced fading due to multipath can occur at lower elevation angles (5° to 30°) where forward scattering from relatively smooth rolling terrain can be received from larger distances.

FIGURE 10

Best fit cumulative fade distributions for multipath fading on tree-lined roads

Curves A: 870 MHz
B: 1.5 GHz
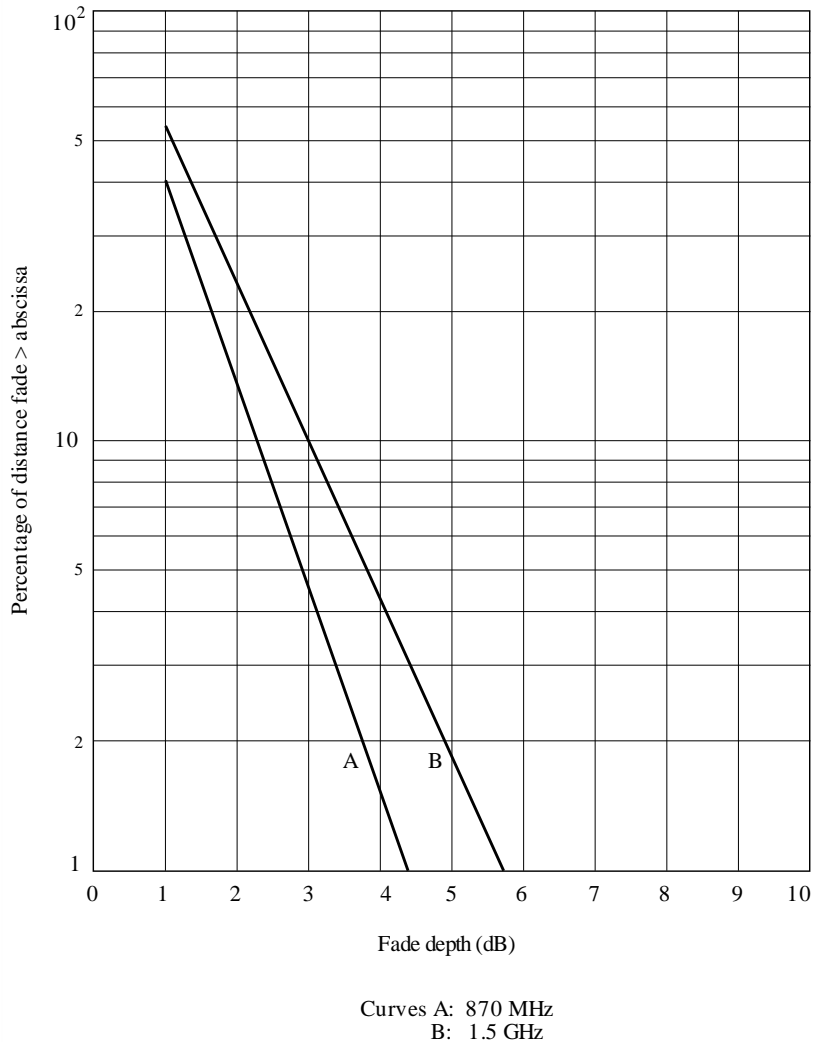
P.0681-10

6   Statistical model for mixed propagation conditions

In §§ 4.1 and 5, models for specific conditions, that is, roadside shadowing conditions and clear line-of-sight conditions in a mountain environment and a roadside tree environment are given. In actual LMSS propagation environments such as rural, wooded, urban and suburban areas, a mixture of different propagation conditions can occur. The cumulative distribution function (CDF) of signal levels in such mixed conditions can be calculated based on the following enhanced 2-state model which is composed of a GOOD state, including slightly shadowed conditions, and a BAD state, including more severe shadowed conditions (referred as "statistical model" hereafter). Based on the same analytical assumptions, time/space series of the power signal level complex envelope can be stochastically generated (referred as "generative model" hereafter). Sections 6.1 and 6.2 provide step-by-step methods to implement respectively the statistical and the generative models. Both models are valid for narrow-band LMSS where the frequency response of the channel affects in the same way all the frequencies within the bandwidth of the signal (frequency non-selective channels).

The long-term variations in the received signal may be described by a semi-Markov chain including the two distinct states, GOOD and BAD (see Fig. 11). The duration of each state is considered to be log-normally distributed. The signal in the Good and Bad states follows a Loo distribution. The Loo distribution considers that the received signal is the sum of two components: the direct path signal and the diffuse multipath. The average direct path amplitude is considered to be normally distributed and the diffuse multipath component follows a Rayleigh distribution. The standard deviation of the direct path amplitude and the multipath power are linearly connected to the average direct path amplitude.

FIGURE 11

2-State Semi-Markov chain approach
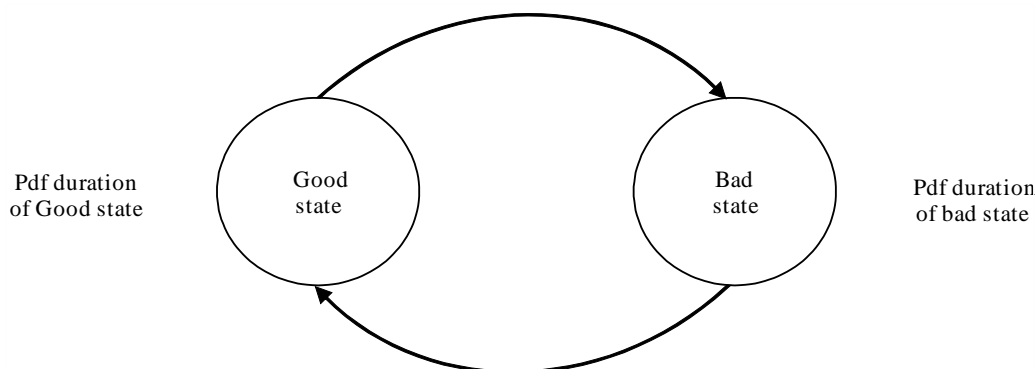
P.0681-11

For the stochastic synthesis of the channel complex envelope, a fixed correlation length for the direct path amplitude should be considered and a fixed Doppler spectrum should be considered for the diffuse multipath component. Between two successive events (belonging necessarily to different states), a given transition length must be considered where the diffuse multipath component power increases/decreases linearly. These transitions should be neglected for the statistical prediction of the channel complex envelope.

The main characteristics of the model are:

1)   The model assumes two states: Good and Bad not necessarily matching with line-of-sight and non-line-of-sight condition.

2)   The duration of each state is characterized by a lognormal distribution:

$$p_{lognormal}(x) = \frac{1}{\sigma_i x \sqrt{\pi}} exp\left[\frac{(lnx - \mu_i)^2}{2\sigma_i^2}\right] \tag{14}$$

where:

$i = G$ for Good states

$i = B$ for Bad states

μ_G and σ_G: mean and standard deviation for Good state

μ_B and σ_B: mean and standard deviation for Bad state

3)   The fading within each state is described by a Loo distribution, where the Loo triplet parameters are not fixed:

Fading~Loo(M_{Ai}, Σ_{Ai}, MP_i),

where:

$i = G$ for Good states

$i = B$ for Bad states

M_{Ai} :   mean of the direct signal

Σ_{Ai} :   standard deviation of the direct signal

MP_i :   mean of the multipath

with:

$M_{Ai} =$ normal(μ_{M_A} , σ_{M_A})

$\Sigma_{Ai} =$ $g_{1i}M_{Ai} + g_{2i}$

$MP_i =$ $h_{1i}M_{Ai} + h_{2i}$

The Loo probability density function is:

$$p_{Loo}(x) = \frac{x \times 8.686}{\Sigma_{Ai}\sigma_i^2 \sqrt{2\pi}} \int_0^\infty \frac{1}{a} \exp\left[-\frac{(20\log_{10}(a) - M_{Ai})^2}{2\Sigma_{Ai}^2} - \frac{x^2 - a^2}{2\sigma_i^2} \right] I_0\left(\frac{xa}{\sigma_i^2} \right) da \tag{15}$$

where

a :   direct signal amplitude

$2\sigma_i^2$:   multipath mean received power, $MP_i = 10\log(2\sigma_i^2)$ dB

3)   The transition length $L_{trans,i}$ between a GOOD and BAD event depends on the $M_{A,i}$ values difference $\Delta M_{A,i} = |M_{A,i\ GOOD} - M_{A,i\ BAD}|$:

$$L_{trans,i} = f_1 \times \Delta M_{A,i} + f_2 \tag{16}$$

In order not to consider unrealistic values for M_A in GOOD and BAD states, restricted probability ranges must be considered:

-    5% − 95% for the GOOD state
-    $[p_{B,min} , p_{B,max}]$ for the BAD state.

In order to consider realistic values for the GOOD and BAD state events duration, minimum possible event lengths must be considered:

-    dur_{minG} for the GOOD state
-    dur_{minB} for the BAD state.

The following input parameters should be used for the statistical and the generative models.

TABLE 5

Model parameters

Parameter	Description
$(\mu,\sigma)_{G,B}$	Mean and standard deviation of the log-normal law assumed for events duration (m)
$dur_{minG,B}$	Minimum possible events duration (m)
$(\mu_{M_A GB}, \sigma_{M_A GB})$	Parameters of the $M_{A\,G,B}$ distribution (M_A being the average value of the direct path amplitude A over one event) (dB)
$MP = h_{1G,B}M_A + h_{2G,B}$	Multipath power, $MP_{G,B,}$ (one 1st order polynomial for each state), (dB)
$\sum_{AG,B} = g_{1G,B}M_A + g_{2G,B}$	Standard deviation of A, $\sum_{A\,G,B}$ (one 1st order polynomial for each state)
$L_{corrG,B}*$	Direct path amplitude correlation distance (m)
$f_1\Delta M_A + f_2$	Transition length, L_{trans} (one single 1st order polynomial), (m)
$[p_{B,min}, p_{B,max}]$	Probability range to consider for the $M_{A\,B}$ distribution

Remark: G stands for the GOOD state and B stands for the BAD state.

* Only for generative modelling.

6.1 Prediction of fading statistics for a single satellite link

The following procedure provides an estimation of overall fading statistics of the LMSS propagation link for frequencies up to 30 GHz with elevation angles from 20° to 90°. However, the suggested parameter values given here limit the applicable frequency range of 1.5 GHz to 20 GHz. The receiving antenna gain assumed here is about 5 dBi for frequencies below 5 GHz and 19 dBi for frequencies above 10 GHz.

Remark: The statistical prediction method has been simplified with respect to the time series synthesis method (§ 6.2) to provide an approximate value of the fading, Rice factor and total power statistics. For better accuracy, statistics must be computed from time series synthesised over 100 km.

Inputs:

– frequency (Hz);

– environment;

– elevation angle.

Step 0: Determine the $(\mu,\sigma)_{G,B}$, (μ_{M_A}, σ_{M_A})$_{G,B}$, $(g_1,g_2)_{G,B}$, $(h_1,h_2)_{G,B}$, $(dur_{min})_{G,B}$, (f_1,f_2), $p_{B,min}$ and $p_{B,max}$ from the input parameters table provided in Annex 2. Consider the table corresponding to the closer elevation angle and frequency to the input values.

Step 1: Calculate the average duration of *GOOD* and *BAD* states, respectively $<dur>_G$ and $<dur>_B$, and the average transition length, $<dur>_T$:

$$\langle dur \rangle_{G,B} = exp\left(\mu_{G,B} + \frac{\sigma_{G,B}^2}{2}\right) \frac{1 - erf\left(\frac{log dur_{min,B,G} - \left(\mu_{G,B} + \sigma_{G,B}^2\right)}{\sigma\sqrt{2}}\right)}{1 - erf\left(\frac{log dur_{min,B,G} - \mu_{G,B}}{\sigma\sqrt{2}}\right)} \qquad (17a)$$

$$\langle dur \rangle_T = f_1 \times \left(\mu_{M_A,G} - \mu_{M_A,B} - \sigma_{M_A,B}^2 \times \frac{p_N\left(M_{A,min}; \mu_{M_A,B}, \sigma_{M_A,B}\right) - p_N\left(M_{A,max}; \mu_{M_A,B}, \sigma_{M_A,B}\right)}{F_N\left(M_{A,max}; \mu_{M_A,B},\right) - F_N\left(M_{A,min}; \mu_{M_A,B}, \sigma_{M_A,B}\right)}\right) + f_2 \qquad (17b)$$

Where

$p_N(x; \mu,\sigma)$ and $F_N(x; \mu,\sigma)$ are respectively the probability density function and the cumulative distribution function of a normal distribution with mean μ and standard deviation σ as defined in Recommendation ITU-R P.1057.

$$M_{A,min,B} = \mu_{M_{AB}} + \sqrt{2}\sigma_{M_{A,B}}erf^{-1}(2p_{B,min} - 1) \tag{18a}$$

$$M_{A,max,B} = \mu_{M_{AB}} + \sqrt{2}\sigma_{M_{A,B}}erf^{-1}(2p_{B,max} - 1) \tag{18b}$$

Step 2: Calculate the probability of GOOD and BAD states p_G and p_B:

$$p_G = \frac{\langle dur\rangle_G + \langle dur\rangle_T}{\langle dur\rangle_G + \langle dur\rangle_B + 2\langle dur\rangle_T} \tag{19a}$$

$$p_B = \frac{\langle dur\rangle_B + \langle dur\rangle_T}{\langle dur\rangle_G + \langle dur\rangle_B + 2\langle dur\rangle_T} \tag{19b}$$

Step 3: Calculate $P(x \leq x_0|GOOD)$ and $P(x \leq x_0|BAD)$ the cumulative distribution of signal level x in GOOD and BAD states as follows:

$$
\begin{aligned}
&P(x \leq x_0|state) \\
&= \frac{2.7647}{\sigma_{M_A}\left(F_N\left(M_{A,max}; \mu_{M_A}, \sigma_{M_A}\right) - F_N\left(M_{A,min}; \mu_{M_A}, \sigma_{M_A}\right)\right)} \int_{M_{A,min}}^{M_{A,max}} \int_0^{x_0} \int_{a_{min}}^{a_{max}} \frac{x}{a(g_1 M_A + g_2)10^{\frac{h_1 M_A + h_2}{10}}} \\
&\times exp\left(-\frac{(M_A - \mu_{M_A})^2}{2\sigma_{M_A}^2} - \frac{(20\log_{10} a - M_A)^2}{2(g_1 M_A + g_2)^2} - \frac{x^2 + a^2}{10^{\frac{h_1 M_A + h_2}{10}}}\right) I_0\left(\frac{2ax}{10^{\frac{h_1 M_A + h_2}{10}}}\right) da\, dx\, dM_A
\end{aligned}
\tag{20a}
$$

where

Parameter	GOOD state	BAD state
$M_{A,min}$	$\mu_{M_{A,G}} - 1.645 \times \sigma_{M_{A,G}}$	$M_{A,min,B}$
$M_{A,max}$	$\mu_{M_{A,G}} + 1.645 \times \sigma_{M_{A,G}}$	$M_{A,max,B}$
a_{min}	$10^{\frac{(1-3g_1)M_A - 3g_2}{20}}$	
a_{max}	$10^{\frac{(1+3g_1)M_A + 3g_2}{20}}$	

Please note that σ_{M_A} may be equal to zero (as for example in the good states of rural and suburban environment for $f = 10 - 20$ GHz). In such condition, M_A is not randomly distributed which changes the expression of the CDF (no integration other than M_a). Then, the cumulative distribution become (with: $M_A = \mu_{M_A}$ here).

$$P(x \leq x_0|state) = \frac{2 \times 8.686}{\sqrt{2\pi}} \int_0^{x_0} \int_{a_{min}}^{a_{max}} \frac{x}{a(g_1 M_A + g_2)10^{\frac{h_1 M_A + h_2}{10}}} \times exp\left(-\frac{(20\log_{10} a - M_A)^2}{2(g_1 M_A + g_2)^2} - \frac{x^2 + a^2}{10^{\frac{h_1 M_A + h_2}{10}}}\right) I_0\left(\frac{2ax}{10^{\frac{h_1 M_A + h_2}{10}}}\right) da\, dx \tag{20b}$$

Step 4: Calculate $P(x \leq x_0)$ the cumulative distribution of signal level x as follows:

$$P(x \leq x_0) = p_G \times P(x \leq x_0|GOOD) + p_B \times P(x \leq x_0|BAD) \tag{21}$$

Step 5: Calculate $P(K \leq K_0|GOOD)$ and $P(K \leq K_0|BAD)$ the cumulative distribution of the Rice factor (dB) K in GOOD and BAD states, as follows:

If $\sigma_{M_A} \neq 0$

$$P(K \leq K_0|state) = \frac{\int_{M_{A,min}}^{M_{A,max}} exp\left(\frac{-(M_A - \mu_{M_A})^2}{2\sigma_{M_A}^2}\right)\left[1 + erf\left(\frac{K_0 - ((1 - h_1)M_A - h_2)}{(g_1 M_A + g_2)\sqrt{2}}\right)\right] dM_A}{\sigma_{M_A}\left(F_N\left(M_{A,max}; \mu_{M_A}, \sigma_{M_A}\right) - F_N\left(M_{A,min}; \mu_{M_A}, \sigma_{M_A}\right)\right)2\sqrt{2\pi}} \tag{22a}$$

If $\sigma_{M_A} = 0$, then

$$P(K \leq K_0|state) = \frac{1 + erf\left(\frac{K_0 - ((1-h_1)M_A - h_2)}{(g_1 M_A + g_2)\sqrt{2}}\right)}{2} \tag{22b}$$

Step 6: Calculate $P(K \leq K_0)$ the cumulative distribution of the Rice factor K, as follows:

$$P(K \leq K_0) = p_G \times P(K \leq K_0|GOOD) + p_B \times P(K \leq K_0|BAD) \tag{23}$$

Step 7: Calculate $P(p_t \leq p_{t,0}|GOOD)$ and $P(p_t \leq p_{t,0}|BAD)$ the cumulative distribution of the total power p_t (direct path power plus diffuse multipath power) in GOOD and BAD states as follows:

For $h_1 \geq 0$:

$$\text{If } \frac{10 log p_{t,0} - h_2}{h_1} < M_{A,min}, P(p_t \leq p_{t,0}|state) = 0 \tag{24a}$$

If $\frac{10 log p_{t,0} - h_2}{h_1} \geq M_{A,min}$ and $\sigma_{M_A} \neq 0$

$P(p_t \leq p_{t,0}|state)$

$$= \frac{\int_{M_{A,min}}^{min\left\{M_{A,max}; \frac{10 log p_{t,0} - h_2}{h_1}\right\}} exp\left(\frac{-(M_A - \mu_{M_A})^2}{2\sigma_{M_A}^2}\right)\left[1 + erf\left(\frac{10 log\left(p_{t,0} - 10^{\frac{h_1 M_A + h_2}{10}}\right) - M_A}{(g_1 M_A + g_2)\sqrt{2}}\right)\right] dM_A}{\sigma_{M_A}\left(F_N\left(M_{A,max}; \mu_{M_A}, \sigma_{M_A}\right) - F_N\left(M_{A,min}; \mu_{M_A}, \sigma_{M_A}\right)\right)2\sqrt{2\pi}} \tag{24b}$$

For $h_1 < 0$:

$$\text{If } \frac{10 log p_{t,0} - h_2}{h_1} > M_{A,max}, P(p_t \leq p_{t,0}|state) = 0 \tag{24c}$$

$$\text{If } \frac{10 log p_{t,0} - h_2}{h_1} \leq M_{A,max} \text{ and } \sigma_{M_A} \neq 0,$$

$$P(p_t \leq p_{t,0}|state) = \frac{\int_{max\left\{M_{A,min}; \frac{10 log p_{t,0} - h_2}{h_1}\right\}}^{M_{A,max}} exp\left(\frac{-(M_A - \mu_{M_A})^2}{2\sigma_{M_A}^2}\right)\left[1 + erf\left(\frac{10 log\left(p_{t,0} - 10^{\frac{h_1 M_A + h_2}{10}}\right) - M_A}{(g_1 M_A + g_2)\sqrt{2}}\right)\right] dM_A}{\sigma_{M_A}\left(F_N\left(M_{A,max}; \mu_{M_A}, \sigma_{M_A}\right) - F_N\left(M_{A,min}; \mu_{M_A}, \sigma_{M_A}\right)\right)2\sqrt{2\pi}} \tag{24d}$$

If $\sigma_{M_A} = 0$, then

$$P(p_t \leq p_{t,0}|state) = \frac{1 + erf\left(\frac{10 log\left(p_{t,0} - 10^{\frac{h_1 M_A + h_2}{10}}\right) - M_A}{(g_1 M_A + g_2)\sqrt{2}}\right)}{2} \tag{24e}$$

Step 8: Calculate $P(p_t \leq p_{t,0})$ the cumulative distribution of the total power p_t as follows:

$$P(p_t \leq p_{t,0}) = p_G \times P(p_t \leq p_{t,0}|_{GOOD}) + p_B \times P(p_t \leq p_{t,0}|_{BAD})$$

(25)

Figures 12, 13 and 14 shows calculated examples of CDFs, for urban and suburban parameters (Europe) at 30 and 60° elevation angle at frequencies between 1.5 and 3 GHz.

FIGURE 12

Calculated examples of fading depth in urban and suburban areas at elevation angles of 30° and 60°
(Europe; 1.5-3 GHz; antenna gain < 5 dBi)

P.0681-12
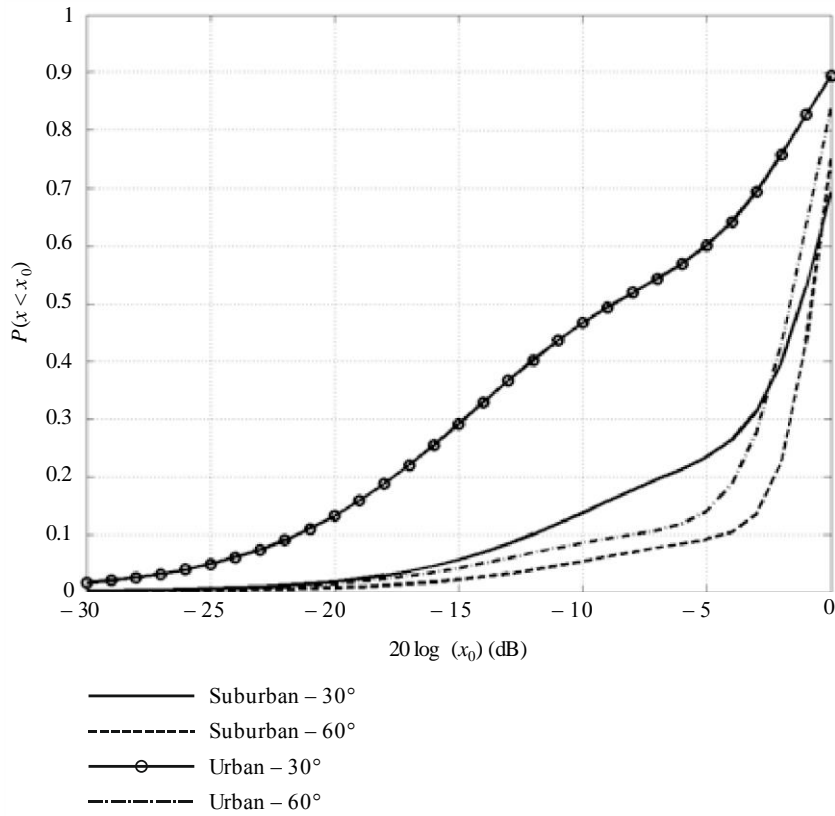
FIGURE 13

**Calculated examples of fading Rice factor in urban and suburban areas at elevation angles of 30° and 60°
(Europe; 1.5-3 GHz; antenna gain < 5 dBi)**

P.0681-13
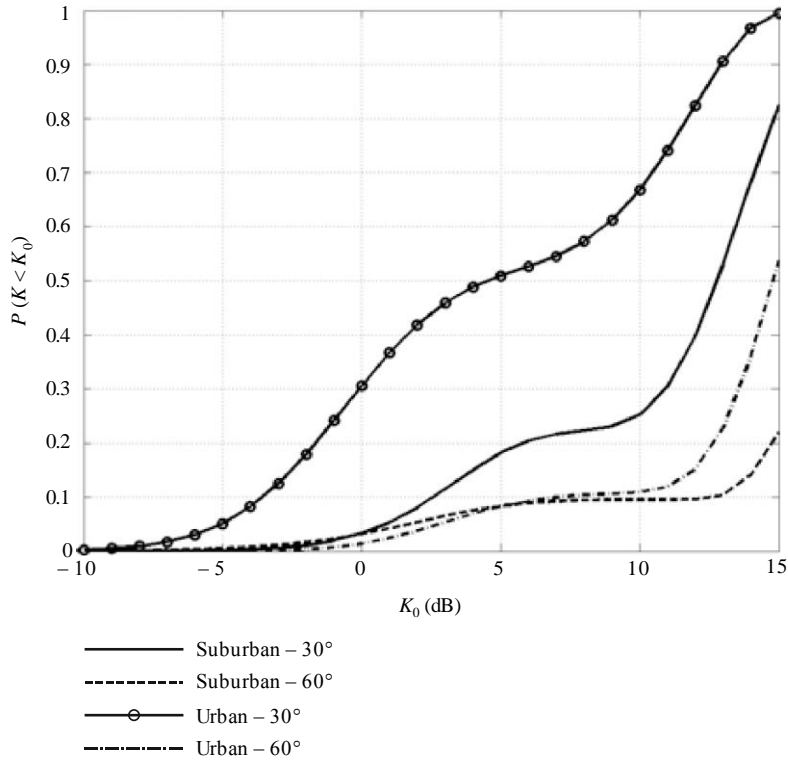
FIGURE 14

**Calculated examples of fading total power in urban and suburban areas at elevation angles of 30° and 60°
(Europe; 1.5-3 GHz; antenna gain < 5 dBi)**
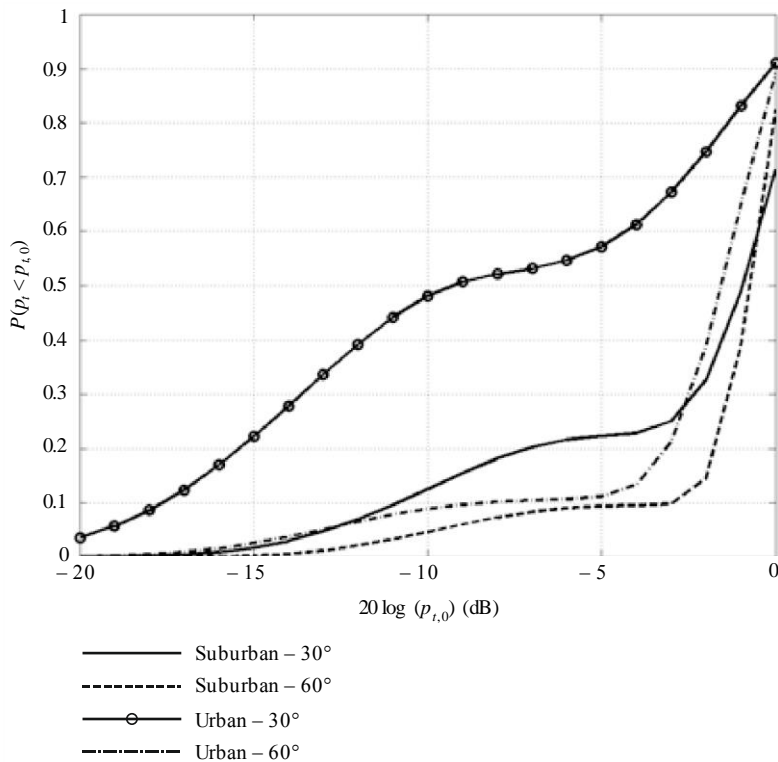
P.0681-14

6.2   Time series synthesis of fading complex envelope

Performance estimation of LMSS receivers requires stochastic synthesis of realistic time series of the channel complex envelope. The semi-Markov enhanced 2-state model should be used to simulate the LMSS time-variations of the channel for a single GSO satellite.

Figure 15 contains the simulator block diagram to generate time/space series of the received power envelope.

FIGURE 15

Simulator block diagram
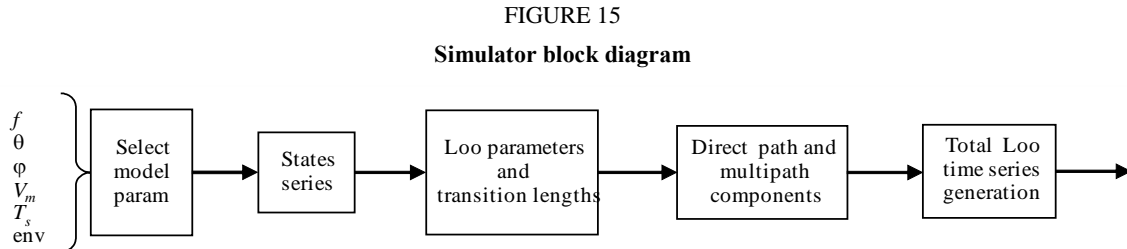
P.0681-15

The step by step generation of the power complex envelope time series is as follows:

Inputs:

–   frequency f (Hz);

–   elevation angle θ (°);

–   azimuth/route orientation φ (°);

–   environment;

–   sampling time T_s (s);

–   mobile speed v_m (m.s^{-1}).

Step 0: Selection of the model parameters $(\mu,\sigma)_{G,B}$, $(\mu_{M_A},\ \sigma_{M_A})_{,B}$, $(g_1,g_2)_{G,B}$, $(h_1,h_2)_{G,B}$, $(dur_{min})_{G,B}$, $(L_{corr})_{G,B}$, f_1, f_2, $conf_{B,min}$, $conf_{B,max}$ depending on the inputs. Consider the table corresponding to the closer elevation angle and frequency to the input values. An example of model parameters is shown in Table 5.

Step 1: Generation of the State Series. A State Series consist of a series of Good events and Bad events. The duration of each event is generated with a lognormal distribution. If a value lower than dur_{min} is drawn, new random draws should be performed until the value is higher than the parameter value.

State_duration$_G$~*lognormal*(μ_G, σ_G)

State_duration$_B$~*lognormal*(μ_B, σ_B)

Figure 16 shows an example of state series, with Good and Bad events of different durations.

FIGURE 16

Example of States Series

State series, semi-Markov
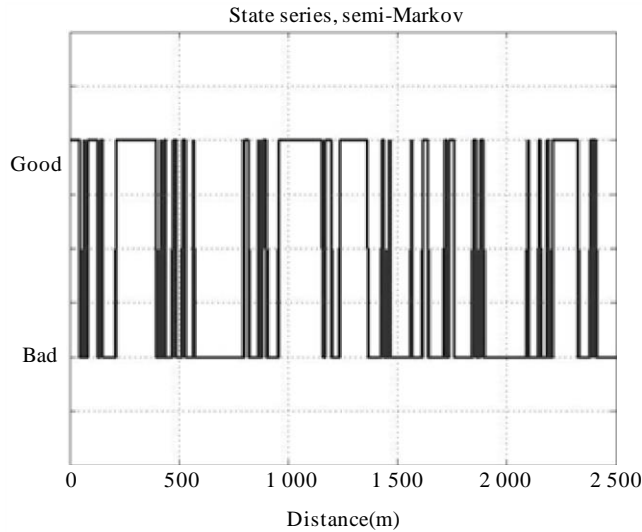
P.0681-16

Step 2: Generation of the Loo parameters triplet (M_A, Σ_A, MP) for each state and the transition lengths (L_{trans}) between states. If a M_A value out of the $[\mu_{M_A,G} - 1.645\sigma_{M_A,G}; \ \mu_{M_A,G} + 1.645\sigma_{M_A,G}]$ range for GOOD state and out of the $[\mu_{M_A,B} + \sqrt{2}\sigma_{M_A,B}erf^{-1}(2p_{B,min} - 1); \ \mu_{M_A,B} + \sqrt{2}\sigma_{M_A,B}erf^{-1}(2p_{B,max} - 1)]$ range for BAD state is drawn, new random draws has to be performed until the value lies into this range.

TABLE 6

Good events	Bad events
$M_{AGi} = \text{Normal}(\mu_{M_A,G}, \sigma_{M_A,G})$	$M_{ABi} = \text{Normal}(\mu_{M_A,B}, \sigma_{M_A,B})$
$\Sigma_{AG\,i} = g_{1G}*M_{AGi} + g_{2G}$	$\Sigma_{AB\,i} = g_{1B}*M_{ABi} + g_{2B}$
$MP_{Gi} = h_{1G}*M_{AGi} + h_{2G}$	$MP_{Bi} = h_{1B}*M_{ABi} + h_{2B}$

Addition of the transition lengths L_{trans} between states (see Fig. 17):

$$L_{trans} = f_1|M_{Ai} - M_{Ai+1}| + f_2 \quad \text{(m)} \tag{26}$$

FIGURE 17

Example of Loo parameters triplet for each states and insertion of transition lengths between states
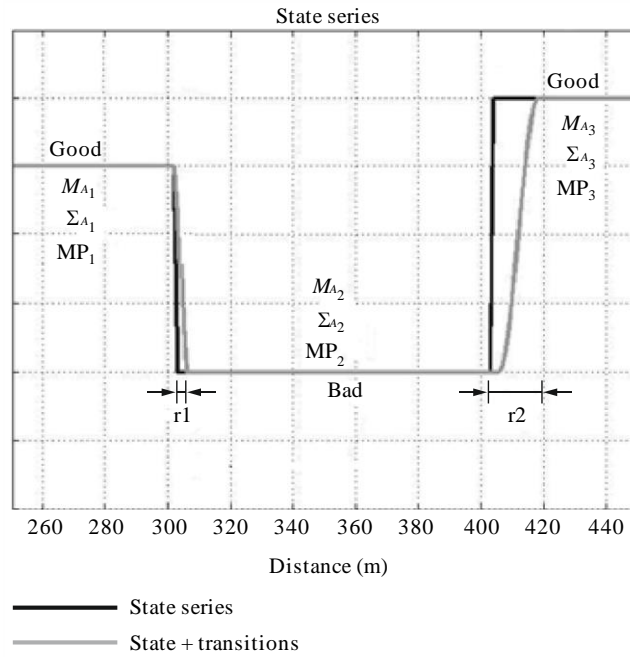
P.0681-17

Step 3: Generation of the Loo total time series

The complex signal variations can be produced using a Loo time series generator. Its implementation is showed in Fig. 18. The parameters of the circuit will be updated for the generations of time series in every state.

Inside a transition, the Loo parameters drawn for the GOOD and BAD states around the transition are interpolated linearly (dB).

FIGURE 18

Loo time series generator
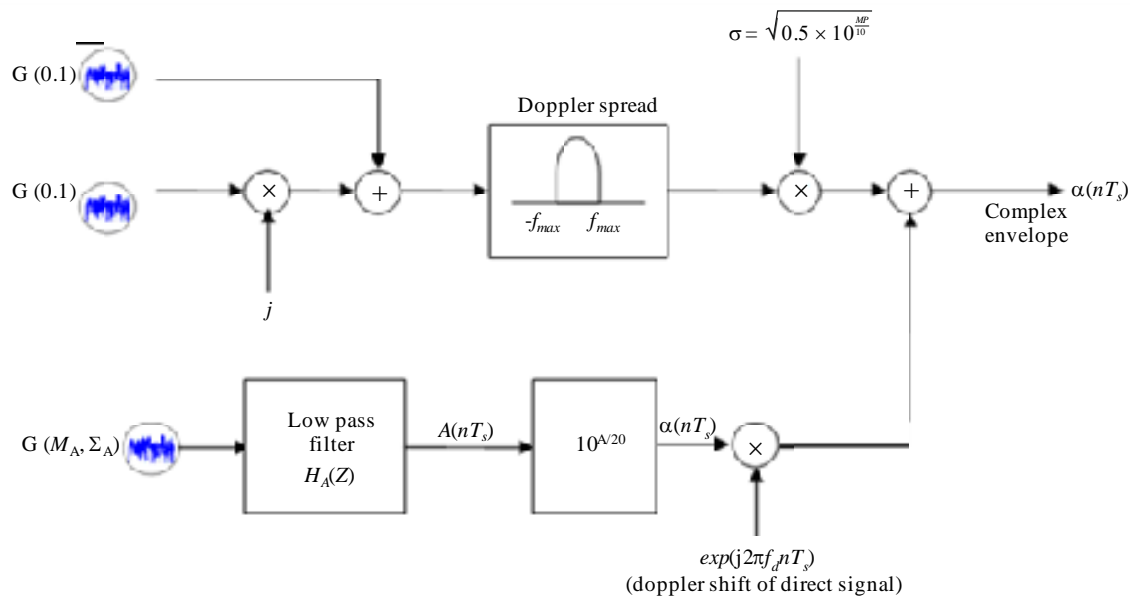
P.0681-18

The upper rail generates the multipath fast variations and the lower rail, the direct signal slow variations.

In the upper rail two zero-mean and unit-standard deviation Gaussian series in quadrature are passed through a unit-energy Doppler filter. After Doppler shaping, the resulting complex series is multiplied by σ, with $2\sigma^2$ being the mean square value of the multipath variations.

The lower rail performs the simulation of the direct signal's amplitude and phase variations. In a first step, a Gaussian distribution with M_A (dB) mean and Σ_A (dB) standard deviation is generated. In a second step, the series, in dB units, is converted to linear units.

In a third step, the phase variations in the direct signal are introduced. These are assumed to be linearly-varying giving rise to a constant Doppler spectral line which depends on the relative mobile-satellite velocity and the angle of arrival, azimuth and elevation, with respect to the mobile trajectory.

The Doppler spectral line frequency is given by:

$$f_d = (f \times v_m / c)\cos\varphi \cdot \cos\theta \tag{27}$$

Fast variations are ruled by the Doppler spread mainly due to the terminal's motion. Depending on the antenna pattern, a Jakes model must be used for generating the fast variations.

The Jakes filter is defined by:

$$\begin{cases} S(f) = \dfrac{K}{\pi f_m \sqrt{1-(f/f_m)^2}} & for \quad |f| < f_m \\ S(f) = 0 & for \quad |f| \geq f_m \end{cases} \tag{28}$$

where $f_m = v_m \times f / c$ and K is a normalisation parameter which ensures that the filtering does not change the process power.

The direct signal's amplitude is subjected to variations slower than those due to multipath caused by shadowing. In this implementation, the rate of change of the slow variations is characterized by the correlation length, L_{corrG} for Good states or L_{corrB} for Bad states. The sampling distance of the multipath being $v_m T_s$, the correlated shadowing time series are generated using the following numerical low pass filter:

$$H_A(Z) = \frac{\sqrt{1-\rho_s^2}}{1-\rho_s Z^{-1}} \text{ with } \rho_s = exp\left(\frac{-v_m T_s}{L_{corr}}\right) \tag{29}$$

Figure 19 shows an example of generated time series (converted into space series).

FIGURE 19

Example of generated space series
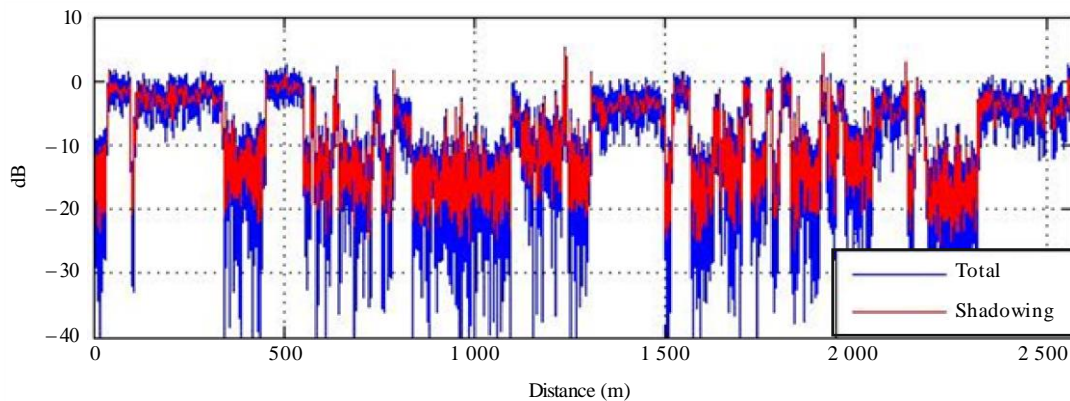
P.0681-19

7 Physical-statistical wideband model for mixed propagation conditions

In § 6, a statistical narrow-band model for LMSS in different environments is given. For broadband LMSS with a multipath propagation channel where different frequencies within the signal bandwidth are affected differently by the channel (frequency-selective channels), a generative model that implements a linear transversal filter whose output is a sum of delayed, attenuated and phase shifted versions of the input signal (wideband model) is more suitable. Definitions on terms related to multipath propagation are found in Recommendation ITU-R P.1407.

The model is given for a situation where a satellite is transmitting from a known position to a receiver on ground, where an elevation ε and an azimuth φ can be computed relative to the receiver heading and position. The model can be applied for frequencies between 1 and 2 GHz and it is valid for wideband systems with a bandwidth up to 100 MHz. The model is based on deterministic and stochastic parameters and it is able to generate vectors that include complex envelope time-series of direct signal and reflections, with corresponding path delay vectors. The parameters determining the stochastic behaviour of the model are derived from measurements obtained on a given scenario. The geometry of the model is based on a synthetic environment representation.

The channel model consists of a combination of the following parts (developed to support the simulation of realistic propagation behaviour for many propagation scenarios of interest, and further validated with empirical analyses based on measured data):

– Shadowing of the direct signal:
  – house front module
  – tree module
  – light pole module
– Reflections module.

The structure of the model is illustrated in Fig. 20 including the following input, intermediate and output time-variant signals:

$v_u(t)$:   user speed

$hd_u(t)$:   user heading

$el_s(t)$:   satellite elevation

$az_s(t)$:   satellite azimuth

$x_u(t)$:   user position in x-axis (y and z axis are considered constant)

$az_u(t)$:   user azimuth

$y_i(t)$:   output signals, where each i is related to direct signal and reflectors.

The propagation mechanisms considered in the model and the synthetic environment are illustrated in Fig. 21.

The model structure is valid for several scenarios: urban vehicle, urban pedestrian, suburban vehicle, suburban pedestrian. The model was developed from measurements on urban and suburban scenarios in and around Munich, Germany. A software with an implementation of the model is available at the Radiocommunication Study Group 3 website. A complete description of the model implementation and usage is provided in a related ITU-R Physical-Statistical Wideband LMSS Model Report available on the ITU-R Study Group website.

FIGURE 20

Structure of the model
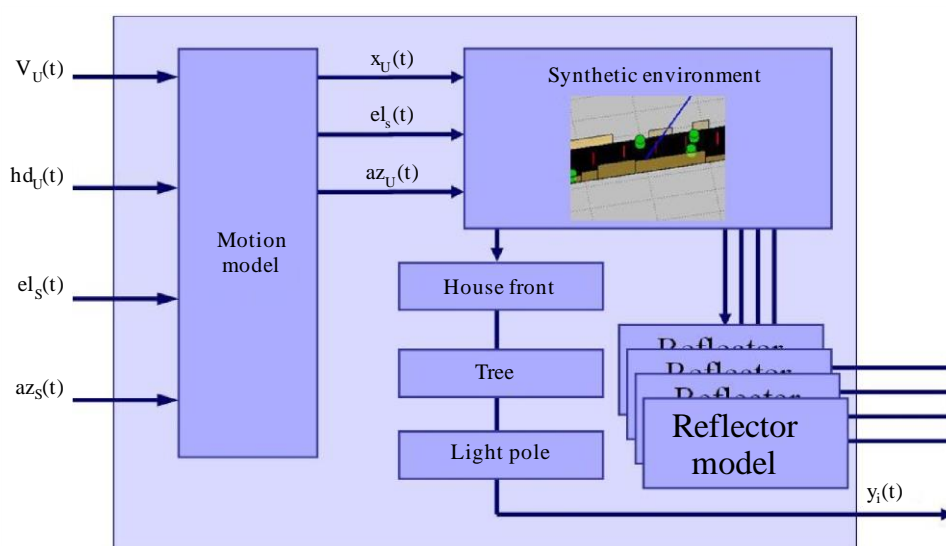
P.0681-20

FIGURE 21

Propagation mechanisms and synthetic environment
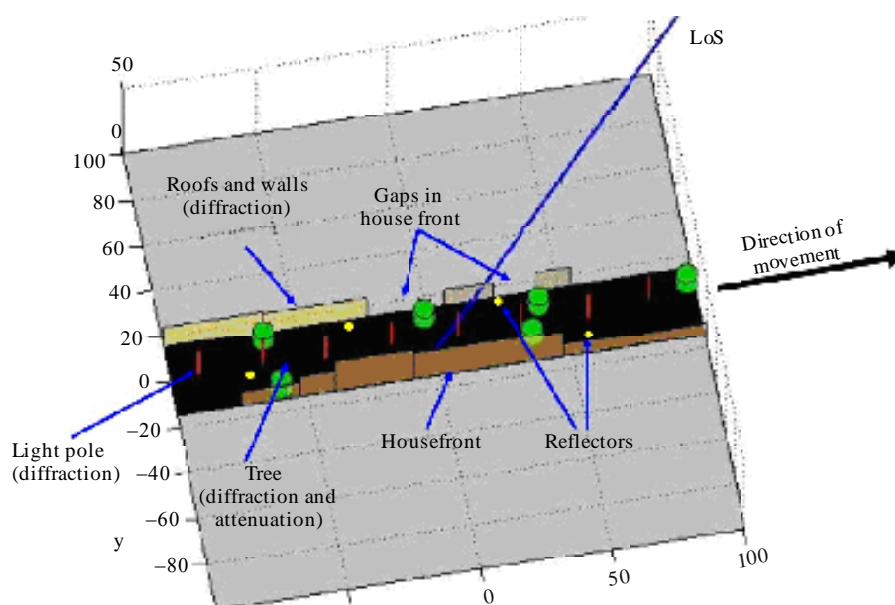
P.0681-21

7.1   Model input

For every input sample some values must be given for the model input:

–   satellite elevation

–   satellite azimuth

–   user speed

–   user heading.

Note that the maximum user speed is limited by the channel impulse response sampling frequency:

$$v < \frac{c_0 f_{samp}}{2 f_c} \tag{30}$$

where:

f_{samp} :   sampling frequency

f_c :   carrier frequency

c_0 :   speed of light.

It is recommended a reasonable over-sampling factor such as 4.

7.2   Model output

The model outputs a vector of N path delays τ_i and N complex values $A_i(t)$ for every time instant. The equivalent baseband channel impulse response is given by:

$$h(t,\tau) = \sum_{i=1}^{N} A_i(t)\delta\left(\tau - \tau_i(t)\right) \tag{31}$$

where t and τ indicate time and delay axes respectively. Note that the path delays $\tau_i(t)$ are time-variant and they can reach arbitrary values.

7.3   Model output usage

Let $s(t)$ be the transmitted equivalent baseband signal, then the received signal $r(t)$ can be calculated in the usual way, by the convolution of the transmitted signal with the channel impulse response as:

$$r(t) = s(t) * h(t, \tau) \tag{32}$$

The channel impulse responses as model output are updated at a rate given by f_{samp} .

8   Wideband satellite-to-indoor channel propagation model

In § 7, a physical-statistical model for wideband simulations has been described that can be applied to land-mobile situations. Within this section, we describe a simulation model that is able to simulate the wideband satellite-to-indoor propagation scenario for receiver algorithm evaluations. In particular, the model supports simulations for communications and for time-of-arrival estimation that is needed in the field of positioning. Similar to § 7, the model provides the parameters of a linear transversal filter that can be used to simulate the frequency-selective fading channel. Definitions on terms related to multipath propagation are found in Recommendation ITU-R P.1407.

The channel model provides simulations for the electromagnetic wave propagation from a satellite based transmitter to a receiver that is located inside a building. A physical-statistical simulation approach has been chosen, i.e. parts of the wave propagation channel are simulated using site specific deterministic methods while other contributions are calculated based on modelled statistics that are obtained from measurements. Measurements in that scope were performed at a carrier frequency of 1.51 GHz with a signal bandwidth of 100 MHz. The transmitter and the environment are assumed to be static or quasi-static while the receiver position may vary with an arbitrary trajectory within a scenery representing a room inside the building. The output will be a set of delays and complex amplitudes for the different multipath components that can be used in a linear transversal filter structure. The obtained parameters of the multipath components change coherently with the receiver positions such that a spatially coherent simulation is supported.

The channel model consists of the following individual components to simulate the propagation channel as illustrated in Fig. 22:

–   Direct components: Representing multipath components that are passing through the outer walls before they are directly received by the receive antenna. These components are based on deterministic calculations using the structure of the scenery.

–   Reflected components: Representing multipath components that are reflected by the interior walls in the scenery. The delay and the angle-of-arrival of these components are simulated using deterministic calculations while the complex amplitude is a stochastic variable.

–   Scattered components: Representing multipath components in a completely stochastic manner. All parameters of these components are simulated as random variables representing interactions of the electromagnetic wave with internal objects like furniture for example.

FIGURE 22

Overview of individual components simulated within the satellite-to-indoor channel model
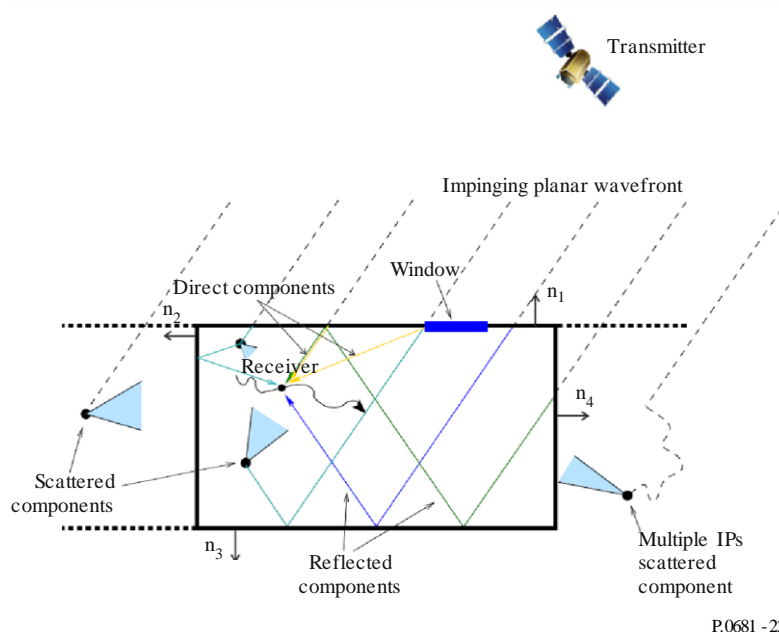
P.0681-22

The model is split into an initialization and runtime phase as displayed in Fig. 23. During the initialization phase the stochastics inside the channel model are initialized such that the runtime phase is completely deterministic based on the drawn random variables. Therefore, the channel impulse response depends only on the receiver position. In order to simulate a certain trajectory of the receiver, the user should call the channel model in the runtime phase repeatedly with new receiver positions in

a loop structure. As input of the channel model for the initialization phase, a description of the scenery, the carrier frequency, the simulation bandwidth, the transmitter position and the root-mean-square (rms) delay spread is expected. Optionally, the number of scattered components may be provided. In terms of propagation parameters, the scenery description includes the perpendicular transmission factors of materials which are the wall material and window glass. Values for the perpendicular transmission coefficient and rms delay spread can be calculated from or found directly in Recommendations ITU-R P.1238 and ITU-R P.2040.

The recommended method is incorporated in a computer program available as Supplement file R-REC-P.681-10-201712-I!!!ZIP.

A complete description of the channel model including its implementation can be found in Report ITU-R P.2145. During the runtime phase, receiver positions need to be supplied by the user within a loop structure.

FIGURE 23

Overview of individual components simulated within the satellite-to-indoor channel model.
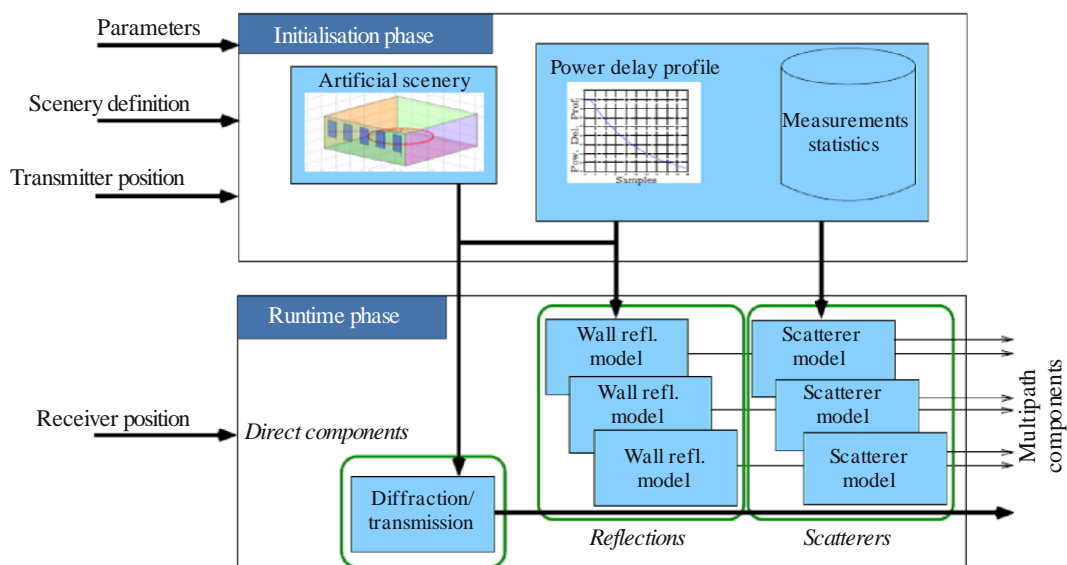
P.0681-23

8.1 Scope of the simulation model

The wideband satellite-to-indoor model is able to simulate a wideband satellite-to-indoor propagation scenario for receiver algorithm evaluations. In particular, the model supports simulations for communications and for time-of-arrival estimation is needed in the field of positioning.

8.2 Applicability of the model

The applicability of the model is limited in the following due to the stochastic parts obtained from measurement data. In its current form, this limits the channel model to the following:

–   Frequency range: 1 GHz to 2 GHz and for signal bandwidth of up to 100 MHz.

–   Polarization: circular polarization.

–   Environment: external facing rooms in typical office environments.

Due to the modelling approach, the wideband satellite-to-indoor model is restricted to:

–   Static transmitter: the transmitter should be static or quasi static during the simulated time period.

–   Room geometry: a single room with at least one wall facing the transmitter.

–   Static environments: the environment is static and the receiver is the only moving object.

–   Negligible outdoor reflections: Outdoor reflections that might occur due to other buildings with similar heights in the vicinity are neglected.

8.3 Input Parameters

During the initialization phase, the wideband satellite-to-indoor channel model requires the following input parameters:

Bandwidth	Signal bandwidth in Hz.
Carrier frequency	Carrier frequency in Hz.
Spatially averaged delay spread	Delay spread in seconds. Delay spread is obtained averaging the power delay profile over simulated space. The parameter defines the slope of the exponential decreasing spatially averaged power delay profile. For delay spread value, a formula and values can be found in Recommendation ITU-R P.1238.
Transmitter position	Three dimensional transmitter position in meters in the simulated reference coordinate system provided by the scenery.
Scenery	Defines the room layout that is needed for the physical deterministic part of the channel model. Additionally, it also incorporates the perpendicular transmission coefficients representing the materials for walls and windows. Appropriate values can be calculated using the single-layer slab method in Recommendation ITU-R P.2040.
Number of scattered components	Optional parameter to change the simulated number of scattered components. The default value is 10 000. Values should be larger than 1 000.

During the runtime phase the wideband satellite-to-indoor channel model, the following inputs are required:

Receiver position	Three dimensional receiver position in meters in the same coordinate system as the transmitter position and the scenery. In order to simulate a certain trajectory of the receiver, the user should call the routine of the channel simulator repeatedly with new receiver positions in a loop structure.

8.4 Output Parameters

The model provides the channel impulse response (CIR) $h(\tau, x_\mathrm{r})$ calculated based on the receiver position x_r provided to the user as:

$$h(\tau, x_\mathrm{r}) = \sum_{l=0}^{L(x_\mathrm{r})-1} \tilde{\alpha}_l(x_\mathrm{r}) \delta(\tau - \tilde{\tau}_l(x_\mathrm{r})), \tag{33}$$

where:

         $L(x_\mathrm{r})$ is the number of visible paths at receiver position x_r

$\tilde{\alpha}_l(x_r)$ is the complex amplitude of the path; it includes already the delay inside the phase

$\tilde{\tau}_l(x_r)$ is the delay in seconds of the path normalized to the line-of-sight propagation time.

9 Satellite diversity

In previous sections single satellite links have been considered. To improve availability, multiple satellite systems may use link diversity. The combination/switching of signals from various satellites is dealt with here. Two cases are considered, namely, the uncorrelated case where it is assumed that shadowing effects affecting received signals from visible satellites are uncorrelated, and the correlated case in which a given degree of correlation is present. In both situations multipath originated signal variations are assumed to be uncorrelated.

9.1 Uncorrelated case

The model in § 6 has a capability for assessing satellite diversity effects in the case of multivisibility satellite constellations (i.e. switching to the least impaired path). For GSO systems, the occurrence probabilities of each state for each satellite link, i.e. P_{GOODn} and P_{BADn} ($n = 1, 2,..., N$; N is number of visible satellites) depend on each satellite elevation θ_n State occurrence probabilities after the state-selection diversity, $P_{GOOD:div}$ and $P_{BAD:div}$ are given by:

$$P_{GOOD:div}=1-\prod_{n=1}^{N}\left[1-P_{GOODn}(\theta_n)\right]$$ (34a)

$$P_{BAD:div} = 1 - P_{GOOD:div}$$ (34b)

In the case of non-GSOs such as LEO and medium Earth orbit (MEO), the occurrence probabilities of the various states for each satellite link vary with time depending on the time-varying satellite elevation. The mean state occurrence probabilities, i.e. $<P_{GOOD:div}>$ and $<P_{BAD:div}>$, after operating satellite diversity from time t_1 to t_2 are as follows:

$$\left\langle P_{i:div} \right\rangle = \frac{1}{t_2 - t_1} \int_{t_1}^{t_2} P_{i:div}(t)\,\mathrm{d}t \qquad (i = GOOD, BAD)$$ (35)

9.2 Correlated case

In many instances, shadowing events affecting two links with a given angle spacing present some degree of correlation that needs to be quantified in order to produce more accurate estimations of the overall availability to be expected in a multiple satellite system. The shadowing cross-correlation coefficient is used for this purpose. This parameter may take up values in the range of ±1 going from positive, close to +1, for small angle spacing to even negative for larger spacing.

9.2.1 Quantification of the shadowing cross-correlation coefficient in urban areas

Here, a simple three-segment model to quantify the cross-correlation coefficient between shadowing events in urban areas is described. A canonical urban area geometry, the "street canyon" is used. The objective is the quantification of the cross-correlation coefficient $\rho(\gamma)$, with γ being the angle spacing between two separate satellite-to-mobile links in street canyons, which are described in terms of their MKA.

The geometry is indicated in Fig. 24 where:

θ_1, θ_2: satellite elevation angle

w: average street width

h: average building height

l: length of street under consideration.

FIGURE 24

Geometry of a street canyon
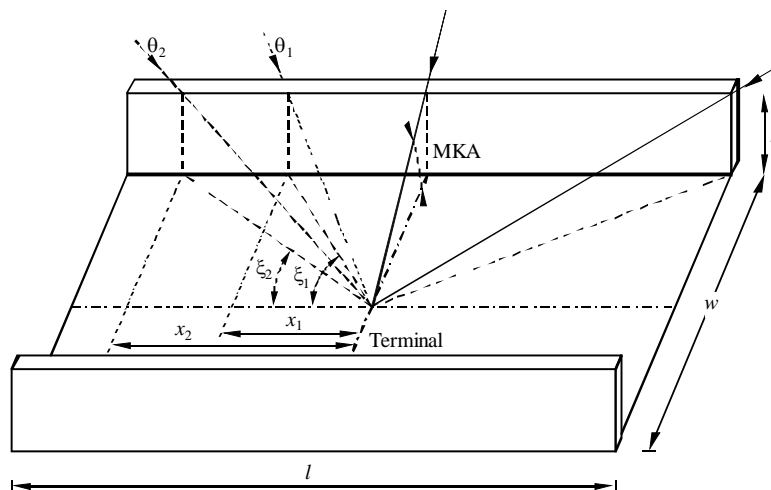
P.0681 -24

The angle spacing between two links, γ, can be put in terms of more convenient angles: the elevations of the two satellites, θ_i and θ_j, and their azimuth spacing, $\Delta\phi$, i.e. the shadowing cross-correlation coefficient can be expressed as $\rho\ (\theta_i, \theta_j, \Delta\phi)$.

Typical results obtained with this model are represented schematically in Fig. 25 which shows a general behaviour with a three-segment pattern defined by points A, B, C and D. In addition to this general pattern, there exist several special cases in which two or more of the four points merge.

Figure 24 shows that, in general, there usually exists a main lobe of positive, decreasing cross-correlation values for small azimuth spacing (typically $\Delta\phi < 30°$) while, for larger values of $\Delta\phi$, the coefficient tends to settle at a constant negative value. The lobe will present higher maxima when the two satellites are at similar elevations. As the difference in elevations increases ($\theta_i \gg \theta_j$), the lobe will show much lower maxima.

FIGURE 25

Three segment cross correlation coefficient model
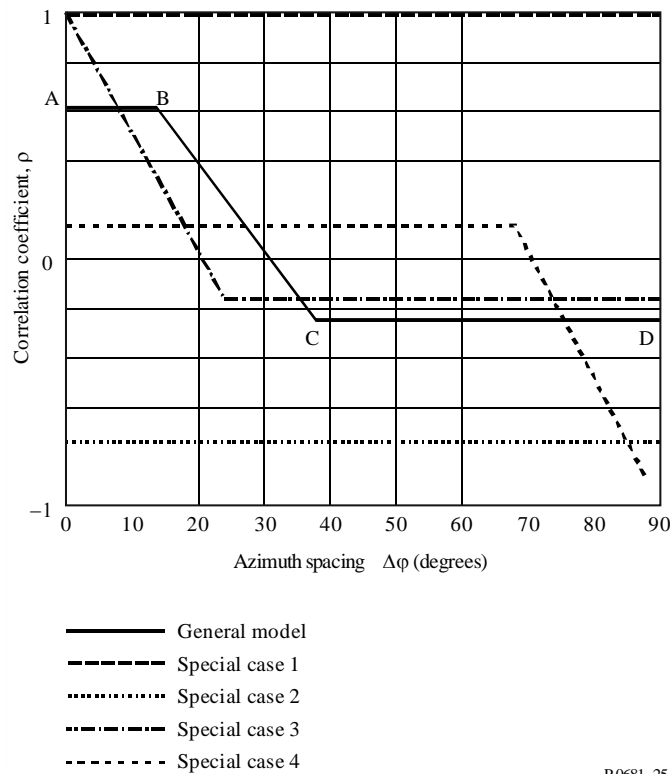
P.0681-25

Special cases of this three-segment model have also been identified: special case 1 occurs when both satellites are above the MKA for any azimuth spacing. In this case, the correlation coefficient takes on a constant positive value of +1 for any $\Delta\varphi$. This is not a relevant case since, in this situation, satellite diversity is not required. Special case 2 occurs when one satellite is always above MKA and the other is always below (except at both ends of the canyon). In this case, the correlation coefficient takes on a constant negative value. Special case 3 occurs when the two satellites are at the same elevation. In this situation, the correlation lobe starts its decay from a maximum value of +1 (i.e. co-located satellites). This special case is applicable to those systems based on GSO satellites, widely spaced in azimuth, but with very similar elevations. Finally, special case 4 occurs for satellites with very different elevations ($\theta_i \gg \theta_j$). Here, the correlation lobe extends across a much wider range of azimuth spacings but showing small positive correlation values.

It must be pointed out that, given the geometry of the scenario (street canyon) and that it is assumed that the user is in the middle of the street, correlation values are symmetric for all four $\Delta\varphi$ quadrants; this is the reason why only one quadrant is shown in Fig. 25.

With reference to Fig. 24, the following input data are used in the model: satellite elevations, θ_1 and θ_2 (degrees), average building height, h (m), average street width, w (m), and length of street under consideration, l (m). A large value is advised for this last parameter, i.e. $l \geq 200$ m. Further, it is assumed that $\theta_2 \geq \theta_1$. The model azimuth spacing, $\Delta\varphi$, resolution is 1° and is valid for all frequency bands although it becomes more accurate for bands above about 10 GHz.

The following steps shall be followed to calculate the cross-correlation coefficient values and azimuth spacings corresponding to model points A, B, C and D:

Step 1: Calculate auxiliary values x_1, x_2, M_1 and M_2 and angles ξ_1 and ξ_2 (see Fig. 24):

$$x_1 = \sqrt{\left(\frac{h}{\tan\theta_1}\right)^2 - \left(\frac{w}{2}\right)^2} \quad \text{and} \quad x_2 = \sqrt{\left(\frac{h}{\tan\theta_1}\right)^2 - \left(\frac{w}{2}\right)^2} \tag{36}$$

–   If $(x_{1,2})^2 < 0$ go to Step 6. This situation occurs when satellite 1 and/or 2 are always in line-of-sight conditions for any azimuth spacing.

–   If $x_{1,2} > l/2$, make $x_{1,2} = l/2$. This situation occurs when there is visibility for satellite 1 and/or 2 only at both ends of the street.

$$\xi_1 = \text{round}\left(\arctan\frac{w/2}{x_1}\right) \quad \text{and} \quad \xi_2 = \text{round}\left(\arctan\frac{w/2}{x_2}\right) \tag{37}$$

$$M_1 = \frac{\xi_1 + 0.5}{90} \quad \text{and} \quad M_2 = \frac{\xi_2 + 0.5}{90} \tag{38}$$

where "round" means rounded to the nearest integer value (degrees).

Step 2: Calculation of auxiliary information related to model points A and D.

For point A:

$$N_{11} = 4\xi_1 + 2 \quad N_{00} = 360 - 4\xi_2 - 2 \quad N_{01} = 4(\xi_2 - \xi_1) \quad N_{10} = 0 \tag{39}$$

For point D:

–   If $\xi_1 + \xi_2 \le 90$,

$$N_{11} = 0 \quad N_{00} = 360 - 4\xi_1 - 4\xi_2 - 4 \quad N_{01} = 4\xi_2 + 2 \quad N_{10} = 4\xi_1 + 2 \tag{40a}$$

–   If $\xi_1 + \xi_2 > 90$,

$$N_{11} = 4\xi_1 + 4\xi_2 + 4 - 360 \quad N_{00} = 0 \quad N_{01} = 360 - 4\xi_1 - 2 \quad N_{10} = 360 - 4\xi_2 - 2 \tag{40b}$$

Step 3: Calculation of the cross-correlation coefficient at points A and D:

$$\rho_{A,D} = \frac{1}{359} \frac{N_{11}(1-M_1)(1-M_2) + N_{00}(0-M_1)(0-M_2) + N_{10}(1-M_1)(0-M_2) + N_{01}(0-M_1)(1-M_2)}{\sigma(\theta_1)\sigma(\theta_2)} \tag{41}$$

$$\sigma^2(\theta_1) = \frac{(4\xi_1 + 2)(1-M_1)^2 + (360 - 4\xi_1 - 2)(0-M_1)^2}{359} \tag{42a}$$

$$\sigma^2(\theta_2) = \frac{(4\xi_2 + 2)(1-M_2)^2 + (360 - 4\xi_2 - 2)(0-M_2)^2}{359} \tag{42b}$$

Step 4: At point B, the correlation coefficient is the same as at point A and its azimuth spacing, $\Delta\varphi$, is given by:

$$\text{Azimuth}_{\text{Point B}} = \xi_2 - \xi_1 \quad\quad \text{degrees} \tag{43}$$

Step 5: At point C, the correlation coefficient is the same as at point D and its azimuth spacing, $\Delta\varphi$, is given by:

–   If $\xi_1 + \xi_2 \le 90$, $\text{Azimuth}_{\text{Point C}} = \xi_1 - \xi_2$ degrees   (44a)

–   If $\xi_1 + \xi_2 > 90$, $\text{Azimuth}_{\text{Point C}} = 180 - \xi_1 - \xi_2$ degrees   (44b)

Step 6: This is the case in which, for one or both elevations, there are always line-of-sight conditions. Here, the correlation coefficient is calculated in a slightly different manner to that in Step 3:

–   If both satellites are always visible, the cross-correlation coefficient is constant and equal to +1 for any $\Delta\varphi$.

–   If one of the satellites is always visible, the cross-correlation coefficient is also constant and is given by:

$$\rho = \left(\frac{N_{11}}{180} - 1 \right) \tag{45}$$

where $N_{11} = 4\xi_1 + 2$, and ξ_1 is calculated as in Step 1.

9.2.2   Availability calculations

Once the cross-correlation coefficient is available, it is possible to compute the availability improvement introduced by the use of satellite diversity. Here, expressions to calculate the system availability for the two-satellite diversity case are provided. Given the usually small margins (or power control ranges) used in land mobile satellite systems, only shadowing effects need to be considered. This is a reasonable working hypothesis since availability events will correspond to links in line-of-sight conditions in which case multipath-originated variations are Ricean and thus, fairly small. In the case of shadowed conditions (heavy or light), the links will be in an outage state even if multipath gives rise to significant signal enhancements.

Given two angle spaced links with unavailability probabilities, p_1 and p_2, and a shadowing cross-correlation coefficient ρ, the overall availability improbability after satellite diversity is given by:

$$p_0 = \rho \sqrt{p_1(1 - p_1)} \sqrt{p_1(1 - p_2)} + p_1\, p_2 \tag{46}$$

and the probability of availability will be $1 - p_0$. Valid values of ρ in equation (46) are limited to those rendering non-negative values for p_0. Probabilities p_1 and p_2, for urban areas can be computed by using the model given in § 4.2.

Overall calculations for a given time interval or for a complete constellation period require the computation of weighted averages over all positions (azimuths and elevations) of the two satellites with respect to the user terminal.

9.3   Modelling satellite diversity effects using MKFs

MKFs as defined in § 4.4 can be used in the calculation of multi-satellite availabilities. Possible partial correlation of blockage effects between the various links is already contained in the geometry of the masks themselves. In Fig. 26 the calculation of the availability of a system comprising two GSO satellites is illustrated. Lines A-B and C-D indicate the sweep paths to be followed for the calculation of the combined availability. Line A-B indicates the 360° azimuth sweep at elevation θ_1 corresponding to satellite-1 and line C-D indicates the 360° azimuth sweep at elevation θ_2 for

satellite-2. To account for the possible blockage cross-correlation the 360° sweep must be carried out preserving the azimuth spacing, Δφ, between the two satellites.

The use of the street MKFs can also be extended to multiple GSO satellites and to the case of non-GSO constellations. In the last case, the study would consist in the repeated computation of 360° street orientation sweeps for a sufficiently large number of satellite constellation snapshots. A snapshot in this context indicates the instantaneous positions (azimuths and elevations) of the various satellites above a minimum operational elevation, θ_min. By defining an appropriate stepping interval, ΔT, and observation period, T_obs, the availability can be can be calculated as the time-, street orientation-weighed average of the obtained results in each snapshot. Values of ΔT = 1 min and T_obs equal to the constellation period provide adequate results.

FIGURE 26

**Calculation of total system availability for a constellation
of two GSO satellites with respect to a T-junction**
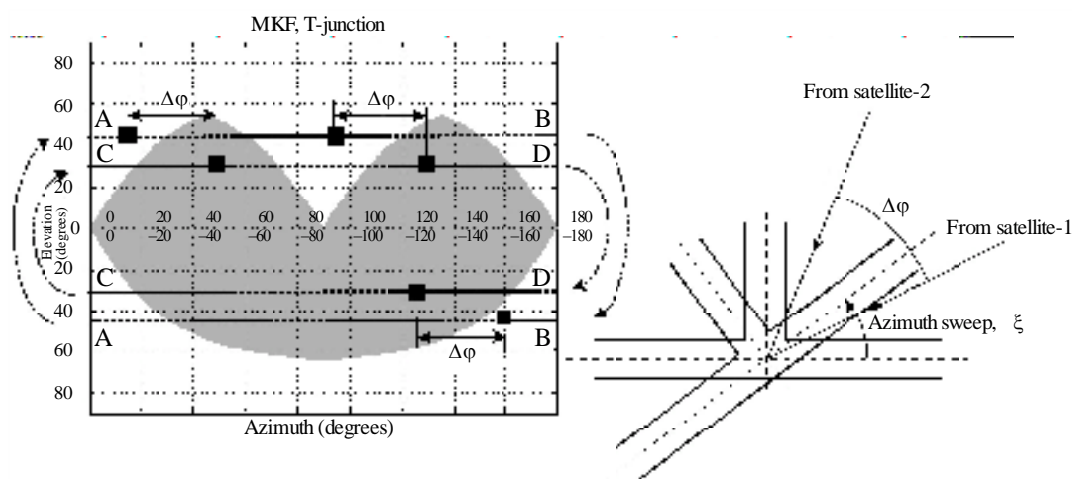
P.0681 -26

Annex 2

1 Introduction

Input parameters for the statistical and generative narrowband models described in § 6 of Annex 1 are provided hereafter for various ranges of frequencies and environments. Available parameters sets are summarized in Tables 7 to 10.

The parameters are presented following the format of Table 7:

TABLE 7

Input parameters data format

Frequency/ environment/ elevation angle (degrees)		
Information	**Useful details about the area or the device used for the channel characterization**	
Parameter	**Good**	**Bad**
$(\mu,\sigma)_{G,B}$	μ_G, σ_G	μ_B, σ_B
$dur_{minG,B}$	dur_{minG}	dur_{minB}
$(\mu_{M_A\,GB}, \sigma_{M_A\,GB})$	$\mu_{M_A}G, \sigma_{M_A}G$	$\mu_{M_A}B, \sigma_{M_A}B$
$MP_{G,B}$	h_{1G}, h_{2G}	h_{1B}, h_{2B}
$\Sigma_{AG,B}$	g_{1G}, g_{2G}	$g_{1B}, g_{2,B}$
$L_{corrG,B}*$	L_{corrG}	$L_{corr,B}$
$f_1\Delta M_A + f_2$	f_1, f_2	
$[p_{B,min}, p_{B,max}]$	Probability range to consider for the $M_{A\,B}$ distribution	

Remark: G stands for the GOOD state and B stands for the BAD state.

* Only for generative modeling.

TABLE 8

Model parameters for frequencies between 1.5 and 3 GHz

Environment	Elevation angle (degrees)				
Urban	20	30	45	60	70
Suburban	20	30	45	60	70
Village	20	30	45	60	70
Rural wooded	20	30	45	60	70
Residential	20	30	–	60	70

TABLE 9

Model parameters for frequencies between 3 and 5 GHz

Environment	Elevation angle (degrees)				
Urban	20	30	45	60	70
Suburban	20	30	45	60	70
Village	20	30	45	60	70
Rural wooded	20	30	45	60	70
Residential	20	30	–	60	70

TABLE 10

Model parameters for frequencies between 10 and 20 GHz

Environment	Elevation angle (degrees)
Suburban	34
Rural	34

2 Frequencies between 1.5 and 3 GHz

2.1 Urban environment

2.2 GHz/ Urban/ 20°		
Information	**Antenna gain < 5 dBi / Measurements performed with an helicopter in and around a typical medium-sized city in France**	
Parameter	**GOOD**	**BAD**
$\mu_{G,B}, \sigma_{G,B}$	2.0042 1.2049	3.689 0.9796
$dur_{minG,B}$	3.9889	10.3114
$\mu_{M_A GB}, \sigma_{M_A GB}$	−3.3681 3.3226	−18.1771 3.2672
$h_{1G,B}, h_{2G,B}$	0.1739 −11.5966	1.1411 4.0581
$g_{1G,B}, g_{2G,B}$	0.0036 1.3230	−0.2502 −1.2528
$L_{corrG,B}$	0.9680	0.9680
$f_1\Delta M_A + f_2$	0.0870 2.8469	
$[p_{B,min}, p_{B,max}]$	[0.1 ; 0.9]	

2.2 GHz/ Urban/ 30°		
Information	**Antenna gain < 5 dBi / Measurements performed with an helicopter in and around a typical medium-sized city in and around a typical medium-sized city in France**	
Parameter	**GOOD**	**BAD**
$\mu_{G,B}, \sigma_{G,B}$	2.7332 1.1030	2.7582 1.2210
$dur_{minG,B}$	7.3174	5.7276
$\mu_{M_A GB}, \sigma_{M_A GB}$	−2.3773 2.1222	−17.4276 3.9532
$h_{1G,B}, h_{2G,B}$	0.0941 −13.1679	0.9175 −0.8009
$g_{1G,B}, g_{2G,B}$	−0.2811 0.9323	−0.1484 0.5910
$L_{corrG,B}$	1.4731	1.4731
$f_1 \Delta M_A + f_2$	0.1378 3.3733	
$[p_{B,min}, p_{B,max}]$	[0.1 ; 0.9]	

2.2 GHz/ Urban/ 45°		
Information	**Antenna gain < 5 dBi / Measurements performed with an helicopter in and around a typical medium-sized city in France**	
Parameter	**GOOD**	**BAD**
$\mu_{G,B}, \sigma_{G,B}$	3.0639 1.6980	2.9108 1.2602
$dur_{minG,B}$	10.0	6.0
$\mu_{M_A GB}, \sigma_{M_A GB}$	−1.8225 1.1317	−15.4844 3.3245
$h_{1G,B}, h_{2G,B}$	−0.0481 −14.7450	0.9434 −1.7555
$g_{1G,B}, g_{2G,B}$	−0.4643 0.3334	−0.0798 2.8101
$L_{corrG,B}$	1.7910	1.7910
$f_1 \Delta M_A + f_2$	0.0744 2.1423	
$[p_{B,min}, p_{B,max}]$	[0.1 ; 0.9]	

2.2 GHz/ Urban/ 60°		
Information	**Antenna gain < 5 dBi / Measurements performed with an helicopter in and around a typical medium-sized city in France**	
Parameter	**GOOD**	**BAD**
$\mu_{G,B}, \sigma_{G,B}$	2.8135 1.5962	2.0211 0.6568
$dur_{minG,B}$	10.0	1.9126
$\mu_{M_A GB}, \sigma_{M_A GB}$	−1.5872 1.2446	−14.1435 3.2706
$h_{1G,B}, h_{2G,B}$	−0.5168 −17.4060	0.6975 −7.5383
$g_{1G,B}, g_{2G,B}$	−0.1953 0.5353	0.0422 3.2030
$L_{corrG,B}$	1.7977	1.7977
$f_1 \Delta M_A + f_2$	−0.1285 5.4991	
$[p_{B,min}, p_{B,max}]$	[0.1 ; 0.9]	

2.2 GHz/ Urban/ 70°		
Information	**Antenna gain < 5 dBi / Measurements performed with an helicopter in and around a typical medium-sized city in France**	
Parameter	**GOOD**	**BAD**
$\mu_{G,B}, \sigma_{G,B}$	4.2919 2.4703	2.1012 1.0341
$dur_{minG,B}$	118.3312	4.8569
$\mu_{M_A GB}, \sigma_{M_A GB}$	−1.8434 0.5370	−12.9383 1.7588
$h_{1G,B}, h_{2G,B}$	−4.7301 −26.5687	2.5318 16.8468
$g_{1G,B}, g_{2G,B}$	0.5192 1.9583	0.3768 8.4377
$L_{corrG,B}$	2.0963	2.0963
$f_1 \Delta M_A + f_2$	−0.0826 2.8824	
$[p_{B,min}, p_{B,max}]$	[0.1 ; 0.9]	

2.2   Suburban environment

2.2 GHz/ Suburban/ 20°		
Information	**Antenna gain < 5 dBi / Measurements performed with an helicopter in and around a typical medium-sized city in France**	
Parameter	**GOOD**	**BAD**
$\mu_{G,B}, \sigma_{G,B}$	2.2201 1.2767	2.2657 1.3812
$dur_{minG,B}$	2.2914	2.5585
$\mu_{M_A GB}, \sigma_{M_A GB}$	−2.7191 1.3840	−13.8808 2.5830
$h_{1G,B}, h_{2G,B}$	−0.3037 −13.0719	1.0136 0.5158
$g_{1G,B}, g_{2G,B}$	−0.1254 0.7894	−0.1441 0.7757
$L_{corrG,B}$	0.9290	0.9290
$f_1 \Delta M_A + f_2$	0.2904 1.0324	
$[p_{B,min}, p_{B,max}]$	[0.1 ; 0.9]	

2.2 GHz/ Suburban/ 30°		
Information	**Antenna gain < 5 dBi / Measurements performed with an helicopter in and around a typical medium-sized city in France**	
Parameter	**GOOD**	**BAD**
$\mu_{G,B}, \sigma_{G,B}$	3.0138 1.4161	2.4521 0.7637
$dur_{minG,B}$	8.3214	5.9087
$\mu_{M_A GB}, \sigma_{M_A GB}$	−0.7018 1.2107	−11.9823 3.4728
$h_{1G,B}, h_{2G,B}$	−0.6543 −14.6457	0.6200 −7.5485
$g_{1G,B}, g_{2G,B}$	−0.1333 0.8992	−0.1644 0.2762
$L_{corrG,B}$	1.7135	1.7135
$f_1 \Delta M_A + f_2$	0.1091 3.3000	
$[p_{B,min}, p_{B,max}]$	[0.1 ; 0.9]	

2.2 GHz/ Suburban/ 45°		
Information	**Antenna gain < 5 dBi / Measurements performed with an helicopter in and around a typical medium-sized city in France**	
Parameter	**GOOD**	**BAD**
$\mu_{G,B}, \sigma_{G,B}$	4.5857 1.3918	2.2414 0.7884
$dur_{minG,B}$	126.8375	4.3132
$\mu_{M_A GB}, \sigma_{M_A GB}$	−1.1496 1.0369	−10.3806 2.3543
$h_{1G,B}, h_{2G,B}$	0.2148 −17.8462	0.0344 −14.2087
$g_{1G,B}, g_{2G,B}$	0.0729 1.0303	0.0662 3.5043
$L_{corrG,B}$	3.2293	3.2293
$f_1 \Delta M_A + f_2$	0.5766 0.7163	
$[p_{B,min}, p_{B,max}]$	[0.1 ; 0.9]	

2.2 GHz/ Suburban/ 60°		
Information	**Antenna gain < 5 dBi / Measurements performed with an helicopter in and around a typical medium-sized city in France**	
Parameter	**GOOD**	**BAD**
$\mu_{G,B}, \sigma_{G,B}$	3.4124 1.4331	1.9922 0.7132
$dur_{minG,B}$	19.5431	3.1213
$\mu_{M_A GB}, \sigma_{M_A GB}$	−0.7811 0.7979	−12.1436 3.1798
$h_{1G,B}, h_{2G,B}$	−2.1102 −19.7954	0.4372 −8.3651
$g_{1G,B}, g_{2G,B}$	−0.2284 0.2796	−0.2903 −0.6001
$L_{corrG,B}$	2.0215	2.0215
$f_1 \Delta M_A + f_2$	−0.4097 8.7440	
$[p_{B,min}, p_{B,max}]$	[0.1 ; 0.9]	

2.2 GHz/ Suburban/ 70°		
Information	**Antenna gain < 5 dBi / Measurements performed with an helicopter in and around a typical medium-sized city in France**	
Parameter	**GOOD**	**BAD**
$\mu_{G,B}, \sigma_{G,B}$	4.2919 2.4703	2.1012 1.0341
$dur_{minG,B}$	118.3312	4.8569
$\mu_{M_A GB}, \sigma_{M_A GB}$	−1.8434 0.5370	−12.9383 1.7588
$h_{1G,B}, h_{2G,B}$	−4.7301 −26.5687	2.5318 16.8468
$g_{1G,B}, g_{2G,B}$	0.5192 1.9583	0.3768 8.4377
$L_{corrG,B}$	2.0963	2.0963
$f_1 \Delta M_A + f_2$	−0.0826 2.8824	
$[p_{B,min}, p_{B,max}]$	[0.1 ; 0.9]	

2.3 Village environment

2.2 GHz/ Village/ 20°		
Information	**Antenna gain < 5 dBi / Measurements performed with an helicopter in and around a typical medium-sized city in France**	
Parameter	**GOOD**	**BAD**
$\mu_{G,B}, \sigma_{G,B}$	2.7663 1.1211	2.2328 1.3788
$dur_{minG,B}$	6.5373	2.8174
$\mu_{M_A GB}, \sigma_{M_A GB}$	−2.5017 2.3059	−15.2300 5.0919
$h_{1G,B}, h_{2G,B}$	0.0238 −11.4824	0.9971 0.8970
$g_{1G,B}, g_{2G,B}$	−0.2735 1.3898	−0.0568 1.9253
$L_{corrG,B}$	0.8574	0.8574
$f_1 \Delta M_A + f_2$	0.0644 2.6740	
$[p_{B,min}, p_{B,max}]$	[0.1 ; 0.9]	

2.2 GHz/ Village/ 30°		
Information	**Antenna gain < 5 dBi / Measurements performed with an helicopter in and around a typical medium-sized city in France**	
Parameter	**GOOD**	**BAD**
$\mu_{G,B}, \sigma_{G,B}$	2.4246 1.3025	1.8980 1.0505
$dur_{minG,B}$	5.4326	2.4696
$h_{1G,B}, h_{2G,B}$	−2.2284 1.4984	−15.1583 4.0987
$g_{1G,B}, g_{2G,B}$	−0.3431 −14.0798	0.9614 0.3719
$h_{1G,B}, h_{2G,B}$	−0.2215 1.0077	−0.0961 1.3123
$L_{corrG,B}$	0.8264	0.8264
$f_1 \Delta M_A + f_2$	−0.0576 3.3977	
$[p_{B,min}, p_{B,max}]$	[0.1 ; 0.9]	

2.2 GHz/ Village/ 45°		
Information	**Antenna gain < 5 dBi / Measurements performed with an helicopter in and around a typical medium-sized city in France**	
Parameter	**GOOD**	**BAD**
$\mu_{G,B}, \sigma_{G,B}$	2.8402 1.4563	1.8509 0.8736
$dur_{minG,B}$	10.4906	2.6515
$\mu_{M_AGB}, \sigma_{M_AGB}$	−1.2871 0.6346	−12.6718 3.1722
$h_{1G,B}, h_{2G,B}$	−0.0222 −16.7316	0.8329 −3.9947
$g_{1G,B}, g_{2G,B}$	−0.3905 0.4880	−0.0980 1.3381
$L_{corrG,B}$	1.4256	1.4256
$f_1\Delta M_A+f_2$	−0.0493 5.3952	
$[p_{B,min}, p_{B,max}]$	[0.1 ; 0.9]	

2.2 GHz/ Village/ 60°		
Information	**Antenna gain < 5 dBi / Measurements performed with an helicopter in and around a typical medium-sized city in France**	
Parameter	**GOOD**	**BAD**
$\mu_{G,B}, \sigma_{G,B}$	3.7630 1.2854	1.7192 1.1420
$dur_{minG,B}$	17.6726	2.5981
$\mu_{M_AGB}, \sigma_{M_AGB}$	−0.5364 0.6115	−9.5399 2.0732
$h_{1G,B}, h_{2G,B}$	−0.1418 −17.8032	−0.4454 −16.8201
$g_{1G,B}, g_{2G,B}$	−0.2120 0.7819	0.0609 2.5925
$L_{corrG,B}$	0.8830	0.8830
$f_1\Delta M_A+f_2$	−0.8818 10.1610	
$[p_{B,min}, p_{B,max}]$	[0.1 ; 0.9]	

2.2 GHz/ Village/ 70°		
Information	**Antenna gain < 5 dBi / Measurements performed with an helicopter in and around a typical medium-sized city in France**	
Parameter	**GOOD**	**BAD**
$\mu_{G,B}, \sigma_{G,B}$	4.0717 1.2475	1.5673 0.5948
$dur_{minG,B}$	30.8829	2.1609
$\mu_{M_AGB}, \sigma_{M_AGB}$	−0.3340 0.6279	−8.3686 2.5603
$h_{1G,B}, h_{2G,B}$	−1.6253 −19.7558	0.1788 −9.5153
$g_{1G,B}, g_{2G,B}$	−0.4438 0.6355	−0.0779 1.1209
$L_{corrG,B}$	1.5633	1.5633
$f_1\Delta M_A+f_2$	−0.3483 5.1244	
$[p_{B,min}, p_{B,max}]$	[0.1 ; 0.9]	

2.4 Rural wooded environment

2.2 GHz/ Rural wooded / 20°		
Information	**Antenna gain < 5 dBi / Measurements performed with an helicopter in and around a typical medium-sized city in France**	
Parameter	**GOOD**	**BAD**
$\mu_{G,B}, \sigma_{G,B}$	2.1597 1.3766	1.9587 1.5465
$dur_{minG,B}$	2.0744	1.3934
$\mu_{M_A GB}, \sigma_{M_A GB}$	−0.8065 1.5635	−10.6615 2.6170
$h_{1G,B}, h_{2G,B}$	−0.9170 −12.1228	0.8440 −1.4804
$g_{1G,B}, g_{2G,B}$	−0.0348 0.9571	−0.1069 1.6141
$L_{corrG,B}$	0.8845	0.8845
$f_1 \Delta M_A + f_2$	0.0550 2.6383	
$[p_{B,min}, p_{B,max}]$	[0.1 ; 0.9]	

2.2 GHz/ Rural wooded / 30°		
Information	**Antenna gain < 5 dBi / Measurements performed with an helicopter in and around a typical medium-sized city in France**	
Parameter	**GOOD**	**BAD**
$\mu_{G,B}, \sigma_{G,B}$	2.5579 1.2444	2.3791 1.1778
$dur_{minG,B}$	3.5947	2.2800
$\mu_{M_A GB}, \sigma_{M_A GB}$	−1.3214 1.6645	−10.4240 2.4446
$h_{1G,B}, h_{2G,B}$	−1.0445 −14.3176	0.6278 −4.8146
$g_{1G,B}, g_{2G,B}$	−0.1656 0.7180	−0.0451 2.2327
$L_{corrG,B}$	1.0942	1.0942
$f_1 \Delta M_A + f_2$	0.0256 3.8527	
$[p_{B,min}, p_{B,max}]$	[0.1 ; 0.9]	

2.2 GHz/ Wooded/ 45°		
Information	**Antenna gain < 5 dBi / Measurements performed with an helicopter in and around a typical medium-sized city in France**	
Parameter	**GOOD**	**BAD**
$\mu_{G,B}, \sigma_{G,B}$	3.1803 1.3427	2.5382 1.1291
$dur_{minG,B}$	6.7673	3.3683
$\mu_{M_A GB}, \sigma_{M_A GB}$	−0.9902 1.0348	−10.2891 2.3090
$h_{1G,B}, h_{2G,B}$	−0.4235 −16.8380	0.3386 −9.7118
$g_{1G,B}, g_{2G,B}$	−0.1095 0.6893	−0.0460 2.1310
$L_{corrG,B}$	2.3956	2.3956
$f_1 \Delta M_A + f_2$	0.2803 4.0004	
$[p_{B,min}, p_{B,max}]$	[0.1 ; 0.9]	

2.2 GHz/ Rural wooded / 60°		
Information	**Antenna gain < 5 dBi / Measurements performed with an helicopter in and around a typical medium-sized city in France**	
Parameter	**GOOD**	**BAD**
$\mu_{G,B}, \sigma_{G,B}$	2.9322 1.3234	2.1955 1.1115
$dur_{minG,B}$	5.7209	1.6512
$\mu_{M_A GB}, \sigma_{M_A GB}$	−0.6153 1.1723	−9.9595 2.2188
$h_{1G,B}, h_{2G,B}$	−1.4024 −16.9664	0.2666 −9.0046
$g_{1G,B}, g_{2G,B}$	−0.2516 0.5353	−0.0907 1.4730
$L_{corrG,B}$	1.7586	1.7586
$f_1 \Delta M_A + f_2$	0.1099 4.2183	
$[p_{B,min}, p_{B,max}]$	[0.1 ; 0.9]	

2.2 GHz/ Rural wooded / 70°		
Information	**Antenna gain < 5 dBi / Measurements performed with an helicopter in and around a typical medium-sized city in France**	
Parameter	**GOOD**	**BAD**
$\mu_{G,B}, \sigma_{G,B}$	3.8768 1.4738	1.8445 0.8874
$dur_{minG,B}$	16.0855	2.9629
$\mu_{M_A GB}, \sigma_{M_A GB}$	−0.7818 0.7044	−6.7769 2.1339
$h_{1G,B}, h_{2G,B}$	−2.9566 −20.0326	−0.3723 −14.9638
$g_{1G,B}, g_{2G,B}$	−0.2874 0.4050	−0.1822 0.1163
$L_{corrG,B}$	1.6546	1.6546
$f_1 \Delta M_A + f_2$	−0.3914 6.6931	
$[p_{B,min}, p_{B,max}]$	[0.1 ; 0.9]	

2.5 Residential environment

2.2 GHz/ Residential/ 20°		
Information	**Antenna gain < 5 dBi / Measurements performed with an helicopter in and around a typical medium-sized city in France**	
Parameter	**GOOD**	**BAD**
$\mu_{G,B}, \sigma_{G,B}$	2.5818 1.7310	1.7136 1.1421
$dur_{minG,B}$	9.2291	1.6385
$\mu_{M_A GB}, \sigma_{M_A GB}$	−0.8449 1.3050	−10.8315 2.2642
$h_{1G,B}, h_{2G,B}$	−0.3977 −12.3714	0.8589 −2.4054
$g_{1G,B}, g_{2G,B}$	0.0984 1.3138	−0.1804 0.8553
$L_{corrG,B}$	1.1578	1.1578
$f_1 \Delta M_A + f_2$	0.0994 2.4200	
$[p_{B,min}, p_{B,max}]$	[0.1 ; 0.9]	

2.2 GHz/ Residential/ 30°		
Information	**Antenna gain < 5 dBi / Measurements performed with an helicopter in and around a typical medium-sized city in France**	
Parameter	**GOOD**	**BAD**
$\mu_{G,B}, \sigma_{G,B}$	3.2810 1.4200	1.8414 0.9697
$dur_{minG,B}$	14.4825	2.7681
$\mu_{M_A GB}, \sigma_{M_A GB}$	−1.3799 1.0010	−11.1669 2.4724
$h_{1G,B}, h_{2G,B}$	−0.8893 −16.4615	−0.1030 −13.7102
$g_{1G,B}, g_{2G,B}$	−0.2432 0.6519	−0.1025 1.7671
$L_{corrG,B}$	1.9053	1.9053
$f_1 \Delta M_A + f_2$	0.0196 3.9374	
$[p_{B,min}, p_{B,max}]$	[0.1 ; 0.9]	

2.2 GHz/ Residential/ 60°		
Information	**Antenna gain < 5 dBi / Measurements performed with an helicopter in and around a typical medium-sized city in France**	
Parameter	**GOOD**	**BAD**
$\mu_{G,B}, \sigma_{G,B}$	3.255 1.287	3.277 1.260
$dur_{minG,B}$	6.47	7.81
$\mu_{M_A GB}, \sigma_{M_A GB}$	0 0.30	−2.32 2.06
$h_{1G,B}, h_{2G,B}$	−2.024 −19.454	−1.496 −22.894
$g_{1G,B}, g_{2G,B}$	0.273 0.403	−0.361 −0.119
$L_{corrG,B}$	3.84	3.84
$f_1 \Delta M_A + f_2$	−1.591 12.274	
$[p_{B,min}, p_{B,max}]$	[0.1 ; 0.9]	

2.2 GHz/ Residential/ 70°		
Information	**Antenna gain < 5 dBi / Measurements performed with an helicopter in and around a typical medium-sized city in France**	
Parameter	**GOOD**	**BAD**
$\mu_{G,B}, \sigma_{G,B}$	4.3291 0.7249	3.4534 0.9763
$dur_{minG,B}$	27.3637	8.9481
$\mu_{M_A GB}, \sigma_{M_A GB}$	−0.1625 0.3249	−1.6084 0.5817
$h_{1G,B}, h_{2G,B}$	0.6321 −21.5594	−0.3976 −22.7905
$g_{1G,B}, g_{2G,B}$	0.1764 0.4135	−0.0796 0.1939
$L_{corrG,B}$	1.6854	1.6854
$f_1\Delta M_A + f_2$	3.0127 6.2345	
$[p_{B,min}, p_{B,max}]$	[0.1 ; 0.9]	

3   Frequencies between 3 and 5 GHz

3.1   Urban environment

3.8 GHz/ Urban/ 20°		
Information	**Antenna gain < 5 dBi / Measurements performed with an helicopter in and around a typical medium-sized city in France**	
Parameter	**GOOD**	**BAD**
$\mu_{G,B}, \sigma_{G,B}$	2.5467 1.0431	3.6890 0.9796
$dur_{minG,B}$	5.2610	10.3114
$\mu_{M_A GB}, \sigma_{M_A GB}$	−2.7844 2.6841	−19.4022 3.2428
$h_{1G,B}, h_{2G,B}$	0.1757 −12.9417	0.9638 −0.9382
$g_{1G,B}, g_{2G,B}$	−0.2044 1.5866	0.0537 4.5670
$L_{corrG,B}$	1.4243	1.4243
$f_1\Delta M_A + f_2$	0.1073 1.9199	
$[p_{B,min}, p_{B,max}]$	[0.1 ; 0.9]	

3.8 GHz/ Urban/ 30°		
Information	**Antenna gain < 5 dBi / Measurements performed with an helicopter in and around a typical medium-sized city in France**	
Parameter	**GOOD**	**BAD**
$\mu_{G,B}, \sigma_{G,B}$	2.0158 1.2348	2.2627 1.4901
$dur_{minG,B}$	4.5491	2.0749
$\mu_{M_A GB}, \sigma_{M_A GB}$	−3.7749 2.2381	−17.9098 2.9828
$h_{1G,B}, h_{2G,B}$	−0.1564 −15.1531	0.8250 −2.5833
$g_{1G,B}, g_{2G,B}$	−0.0343 1.0602	−0.0741 2.1406
$L_{corrG,B}$	0.8999	0.8999
$f_1\Delta M_A + f_2$	0.2707 -0.0287	
$[p_{B,min}, p_{B,max}]$	[0.1 ; 0.9]	

3.8 GHz/ Urban/ 45°		
Information	**Antenna gain < 5 dBi / Measurements performed with an helicopter in and around a typical medium-sized city in France**	
Parameter	**GOOD**	**BAD**
$\mu_{G,B}, \sigma_{G,B}$	2.3005 1.6960	2.6314 1.1210
$dur_{minG,B}$	10.0	6.0
$\mu_{M_A GB}, \sigma_{M_A GB}$	−1.4466 1.1472	−15.3926 3.2527
$h_{1G,B}, h_{2G,B}$	0.1550 −13.6861	0.9509 −1.2462
$g_{1G,B}, g_{2G,B}$	0.1666 1.2558	0.0363 4.4356
$L_{corrG,B}$	1.6424	1.6424
$f_1\Delta M_A + f_2$	0.2517 −0.3512	
$[p_{B,min}, p_{B,max}]$	[0.1 ; 0.9]	

3.8 GHz/ Urban/ 60°		
Information	**Antenna gain < 5 dBi / Measurements performed with an helicopter in and around a typical medium-sized city in France**	
Parameter	**GOOD**	**BAD**
$\mu_{G,B}, \sigma_{G,B}$	2.4546 1.9595	1.8892 0.8982
$dur_{minG,B}$	10.0	1.9126
$\mu_{M_A GB}, \sigma_{M_A GB}$	−1.6655 0.8244	−14.4922 3.4941
$h_{1G,B}, h_{2G,B}$	−0.4887 −17.2505	0.4501 −9.6935
$g_{1G,B}, g_{2G,B}$	−0.3373 0.3285	0.1202 4.8329
$L_{corrG,B}$	2.3036	2.3036
$f_1\Delta M_A + f_2$	0.0025 1.4949	
$[p_{B,min}, p_{B,max}]$	[0.1 ; 0.9]	

3.8 GHz/ Urban/ 70°		
Information	**Antenna gain < 5 dBi / Measurements performed with an helicopter in and around a typical medium-sized city in France**	
Parameter	**GOOD**	**BAD**
$\mu_{G,B}, \sigma_{G,B}$	2.8354 2.4631	1.5170 1.1057
$dur_{minG,B}$	67.5721	3.6673
$\mu_{M_A GB}, \sigma_{M_A GB}$	−1.0455 0.2934	−14.2294 5.4444
$h_{1G,B}, h_{2G,B}$	−3.0973 −20.7862	0.0908 −15.8022
$g_{1G,B}, g_{2G,B}$	0.0808 0.8952	0.0065 3.1520
$L_{corrG,B}$	2.2062	2.2062
$f_1 \Delta M_A + f_2$	0.0755 2.1426	
$[p_{B,min}, p_{B,max}]$	[0.1 ; 0.9]	

3.2   Suburban environment

3.8 GHz/ Suburban/ 20°		
Information	**Antenna gain < 5 dBi / Measurements performed with an helicopter in and around a typical medium-sized city in France**	
Parameter	**GOOD**	**BAD**
$\mu_{G,B}, \sigma_{G,B}$	2.8194 1.6507	2.5873 1.3919
$dur_{minG,B}$	11.1083	4.4393
$\mu_{M_A GB}, \sigma_{M_A GB}$	−4.8136 1.9133	−17.0970 2.9350
$h_{1G,B}, h_{2G,B}$	−0.4500 -17.9227	0.8991 −2.4082
$g_{1G,B}, g_{2G,B}$	−0.1763 0.8244	0.0582 4.0347
$L_{corrG,B}$	1.2571	1.2571
$f_1 \Delta M_A + f_2$	0.0727 2.8177	
$[p_{B,min}, p_{B,max}]$	[0.1 ; 0.9]	

3.8 GHz/ Suburban/ 30°		
Information	**Antenna gain < 5 dBi / Measurements performed with an helicopter in and around a typical medium-sized city in France**	
Parameter	**GOOD**	**BAD**
$\mu_{G,B}, \sigma_{G,B}$	2.9226 1.3840	2.7375 0.6890
$dur_{minG,B}$	6.7899	7.7356
$h_{1G,B}, h_{2G,B}$	−1.9611 1.8460	−15.3022 2.9379
$g_{1G,B}, g_{2G,B}$	0.2329 −15.0063	0.5146 −8.9987
$h_{1G,B}, h_{2G,B}$	0.0334 1.3323	0.0880 4.4692
$L_{corrG,B}$	1.6156	1.6156
$f_1 \Delta M_A + f_2$	0.1281 2.3949	
$[p_{B,min}, p_{B,max}]$	[0.1 ; 0.9]	

3.8 GHz/ Suburban/ 45°		
Information	Antenna gain < 5 dBi / Measurements performed with an helicopter in and around a typical medium-sized city in France	
Parameter	**GOOD**	**BAD**
$\mu_{G,B}, \sigma_{G,B}$	4.3019 0.8530	2.3715 1.3435
$dur_{minG,B}$	36.1277	9.5511
$\mu_{M_A GB}, \sigma_{M_A GB}$	−1.2730 0.9286	−5.6373 2.9302
$h_{1G,B}, h_{2G,B}$	0.2050 −17.5670	−0.7188 −21.0513
$g_{1G,B}, g_{2G,B}$	0.0074 0.7490	−0.2896 −0.3951
$L_{corrG,B}$	1.1191	1.1191
$f_1\Delta M_A + f_2$	−0.9586 10.8084	
$[p_{B,min}, p_{B,max}]$	[0.1 ; 0.9]	

3.8 GHz/ Suburban/ 60°		
Information	Antenna gain < 5 dBi / Measurements performed with an helicopter in and around a typical medium-sized city in France	
Parameter	**GOOD**	**BAD**
$\mu_{G,B}, \sigma_{G,B}$	2.8958 1.7061	1.9128 0.6869
$dur_{minG,B}$	13.9133	2.9398
$\mu_{M_A GB}, \sigma_{M_A GB}$	−1.1987 1.0492	−13.1811 2.6228
$h_{1G,B}, h_{2G,B}$	−1.6501 −18.9375	0.6911 −6.0721
$g_{1G,B}, g_{2G,B}$	−0.1369 0.4477	0.0598 3.7220
$L_{corrG,B}$	3.0619	3.0619
$f_1\Delta M_A + f_2$	−0.0419 5.8920	
$[p_{B,min}, p_{B,max}]$	[0.1 ; 0.9]	

3.8 GHz/ Suburban/ 70°		
Information	Antenna gain < 5 dBi / Measurements performed with an helicopter in and around a typical medium-sized city in France	
Parameter	**GOOD**	**BAD**
$\mu_{G,B}, \sigma_{G,B}$	4.1684 1.0766	1.4778 0.7033
$dur_{minG,B}$	42.0185	1.8473
$\mu_{M_A GB}, \sigma_{M_A GB}$	0.1600 0.5082	−10.2225 1.8417
$h_{1G,B}, h_{2G,B}$	−3.4369 −18.1632	0.3934 −9.6284
$g_{1G,B}, g_{2G,B}$	−1.1144 0.9703	−0.1331 0.7223
$L_{corrG,B}$	2.5817	2.5817
$f_1\Delta M_A + f_2$	−0.1129 4.0555	
$[p_{B,min}, p_{B,max}]$	[0.1 ; 0.9]	

3.3 Village environment

3.8 GHz/ Village/ 20°		
Information	**Antenna gain < 5 dBi / Measurements performed with an helicopter in and around a typical medium-sized city in France**	
Parameter	**GOOD**	**BAD**
$\mu_{G,B}, \sigma_{G,B}$	2.0262 1.2355	1.9451 1.4293
$dur_{minG,B}$	2.2401	1.9624
$\mu_{M_A GB}, \sigma_{M_A GB}$	−3.1324 1.8929	−16.5697 4.0368
$h_{1G,B}, h_{2G,B}$	−0.4368 −15.1009	1.0921 1.6440
$g_{1G,B}, g_{2G,B}$	−0.0423 1.2532	−0.0325 2.4452
$L_{corrG,B}$	0.8380	0.8380
$f_1 \Delta M_A + f_2$	0.0590 1.5623	
$[p_{B,min}, p_{B,max}]$	[0.1 ; 0.9]	

3.8 GHz/ Village/ 30°		
Information	**Antenna gain < 5 dBi / Measurements performed with an helicopter in and around a typical medium-sized city in France**	
Parameter	**GOOD**	**BAD**
$\mu_{G,B}, \sigma_{G,B}$	2.4504 1.1061	1.7813 1.2802
$dur_{minG,B}$	2.3941	2.1484
$\mu_{M_A GB}, \sigma_{M_A GB}$	−1.8384 1.7960	−15.4143 4.5579
$h_{1G,B}, h_{2G,B}$	−0.5582 −14.4416	0.8549 −2.2415
$g_{1G,B}, g_{2G,B}$	−0.4545 0.8188	−0.0761 1.6768
$L_{corrG,B}$	0.9268	0.9268
$f_1 \Delta M_A + f_2$	−0.0330 2.7056	
$[p_{B,min}, p_{B,max}]$	[0.1 ; 0.9]	

3.8 GHz/ Village/ 45°		
Information	**Antenna gain < 5 dBi / Measurements performed with an helicopter in and around a typical medium-sized city in France**	
Parameter	**GOOD**	**BAD**
$\mu_{G,B}, \sigma_{G,B}$	2.2910 1.4229	1.2738 1.1539
$dur_{minG,B}$	2.8605	0.7797
$\mu_{M_A GB}, \sigma_{M_A GB}$	−0.0018 1.1193	−12.1063 2.9814
$h_{1G,B}, h_{2G,B}$	−1.2023 −14.0732	0.6537 −4.5948
$g_{1G,B}, g_{2G,B}$	−0.1033 0.9299	−0.0815 1.6693
$L_{corrG,B}$	0.9288	0.9288
$f_1 \Delta M_A + f_2$	0.0002 1.9694	
$[p_{B,min}, p_{B,max}]$	[0.1 ; 0.9]	

3.8 GHz/ Village/ 60°		
Information	**Antenna gain < 5 dBi / Measurements performed with an helicopter in and around a typical medium-sized city in France**	
Parameter	**GOOD**	**BAD**
$\mu_{G,B}, \sigma_{G,B}$	3.0956 1.3725	1.0920 1.2080
$dur_{minG,B}$	8.1516	0.7934
$\mu_{M_A GB}, \sigma_{M_A GB}$	−0.5220 1.0950	−12.1817 3.3604
$h_{1G,B}, h_{2G,B}$	0.0831 −16.8546	1.1006 0.5381
$g_{1G,B}, g_{2G,B}$	0.0411 1.1482	−0.0098 2.4287
$L_{corrG,B}$	1.2251	1.2251
$f_1 \Delta M_A + f_2$	−0.0530 2.7165	
$[p_{B,min}, p_{B,max}]$	[0.1 ; 0.9]	

3.8 GHz/ Village/ 70°		
Information	**Antenna gain < 5 dBi / Measurements performed with an helicopter in and around a typical medium-sized city in France**	
Parameter	**GOOD**	**BAD**
$\mu_{G,B}, \sigma_{G,B}$	3.9982 1.3320	1.4165 0.4685
$dur_{minG,B}$	28.3220	2.5168
$\mu_{M_A GB}, \sigma_{M_A GB}$	−1.3403 0.7793	−11.9560 1.5654
$h_{1G,B}, h_{2G,B}$	−0.4861 −19.5316	0.5663 −6.8615
$g_{1G,B}, g_{2G,B}$	−0.2356 0.7178	−0.2903 −1.2715
$L_{corrG,B}$	1.4378	1.4378
$f_1 \Delta M_A + f_2$	−0.0983 3.9005	
$[p_{B,min}, p_{B,max}]$	[0.1 ; 0.9]	

3.4   Rural wooded environment

3.8 GHz/ Rural wooded/ 20°		
Information	**Antenna gain < 5 dBi / Measurements performed with an helicopter in and around a typical medium-sized city in France**	
Parameter	**GOOD**	**BAD**
$\mu_{G,B}, \sigma_{G,B}$	2.0294 1.4280	2.0290 1.5493
$dur_{minG,B}$	1.7836	1.5269
$\mu_{M_A GB}, \sigma_{M_A GB}$	−3.2536 1.6159	−14.3363 2.7753
$h_{1G,B}, h_{2G,B}$	−0.5718 −16.1382	0.8186 −2.9963
$g_{1G,B}, g_{2G,B}$	−0.0805 0.9430	−0.0822 1.7660
$L_{corrG,B}$	1.0863	1.0863
$f_1 \Delta M_A + f_2$	0.1263 1.4478	
$[p_{B,min}, p_{B,max}]$	[0.1 ; 0.9]	

3.8 GHz/ Rural wooded / 30°		
Information	**Antenna gain < 5 dBi / Measurements performed with an helicopter in and around a typical medium-sized city in France**	
Parameter	**GOOD**	**BAD**
$\mu_{G,B}, \sigma_{G,B}$	2.1218 1.4895	2.2051 1.5741
$dur_{minG,B}$	2.4539	2.1289
$\mu_{M_A GB}, \sigma_{M_A GB}$	−1.5431 1.8811	−12.8884 3.0097
$h_{1G,B}, h_{2G,B}$	−0.7288 −14.1626	0.6635 −4.6034
$g_{1G,B}, g_{2G,B}$	−0.1241 0.9482	−0.0634 2.3898
$L_{corrG,B}$	1.3253	1.3253
$f_1 \Delta M_A + f_2$	0.0849 1.6324	
$[p_{B,min}, p_{B,max}]$	[0.1 ; 0.9]	

3.8 GHz/ Rural wooded / 45°		
Information	**Antenna gain < 5 dBi / Measurements performed with an helicopter in and around a typical medium-sized city in France**	
Parameter	**GOOD**	**BAD**
$\mu_{G,B}, \sigma_{G,B}$	3.1803 1.3427	2.4017 1.1315
$dur_{minG,B}$	6.7673	3.5668
$\mu_{M_A GB}, \sigma_{M_A GB}$	0.0428 1.6768	−11.3173 2.7467
$h_{1G,B}, h_{2G,B}$	−0.9948 −14.4265	0.2929 −9.7910
$g_{1G,B}, g_{2G,B}$	−0.1377 1.0077	−0.0387 2.6194
$L_{corrG,B}$	2.0419	2.0419
$f_1 \Delta M_A + f_2$	0.1894 2.1378	
$[p_{B,min}, p_{B,max}]$	[0.1 ; 0.9]	

3.8 GHz/ Rural wooded / 60°		
Information	**Antenna gain < 5 dBi / Measurements performed with an helicopter in and around a typical medium-sized city in France**	
Parameter	**GOOD**	**BAD**
$\mu_{G,B}, \sigma_{G,B}$	2.4961 1.4379	2.2113 1.1254
$dur_{minG,B}$	3.7229	1.9001
$\mu_{M_A GB}, \sigma_{M_A GB}$	−1.0828 1.0022	−12.3044 2.3641
$h_{1G,B}, h_{2G,B}$	−1.2973 −16.6791	0.5456 −6.4660
$g_{1G,B}, g_{2G,B}$	−0.1187 0.6254	−0.0443 2.3029
$L_{corrG,B}$	1.9038	1.9038
$f_1\Delta M_A + f_2$	0.1624 1.8417	
$[p_{B,min}, p_{B,max}]$	[0.1 ; 0.9]	

3.8 GHz/ Rural wooded / 70°		
Information	**Antenna gain < 5 dBi / Measurements performed with an helicopter in and around a typical medium-sized city in France**	
Parameter	**GOOD**	**BAD**
$\mu_{G,B}, \sigma_{G,B}$	2.8382 1.3804	2.1470 1.0038
$dur_{minG,B}$	6.8051	1.9195
$\mu_{M_A GB}, \sigma_{M_A GB}$	−0.8923 0.9455	−11.5722 2.3437
$h_{1G,B}, h_{2G,B}$	−1.3425 −17.5636	0.3459 −9.5399
$g_{1G,B}, g_{2G,B}$	−0.1210 0.6444	−0.0275 2.6238
$L_{corrG,B}$	2.1466	2.1466
$f_1\Delta M_A + f_2$	0.0593 2.8854	
$[p_{B,min}, p_{B,max}]$	[0.1 ; 0.9]	

3.5   Residential environment

3.8 GHz/ Residential/ 20°		
Information	**Antenna gain < 5 dBi / Measurements performed with an helicopter in and around a typical medium-sized city in France**	
Parameter	**GOOD**	**BAD**
$\mu_{G,B}, \sigma_{G,B}$	2.9050 1.7236	2.1969 0.9865
$dur_{minG,B}$	10.7373	2.2901
$\mu_{M_A GB}, \sigma_{M_A GB}$	−1.4426 1.2989	−14.4036 3.0396
$h_{1G,B}, h_{2G,B}$	0.4875 −13.5981	0.5813 −6.9790
$g_{1G,B}, g_{2G,B}$	0.1343 1.8247	−0.0911 2.1475
$L_{corrG,B}$	1.2788	1.2788
$f_1\Delta M_A + f_2$	0.2334 0.7612	
$[p_{B,min}, p_{B,max}]$	[0.1 ; 0.9]	

3.8 GHz/ Residential/ 30°		
Information	Antenna gain < 5 dBi / Measurements performed with an helicopter in and around a typical medium-sized city in France	
Parameter	**GOOD**	**BAD**
$\mu_{G,B}, \sigma_{G,B}$	2.7334 1.6971	1.8403 0.9268
$dur_{minG,B}$	10.2996	1.8073
$\mu_{M_A GB}, \sigma_{M_A GB}$	−0.9996 1.0752	−12.9855 2.8149
$h_{1G,B}, h_{2G,B}$	0.3407 −14.8465	0.3553 −9.9284
$g_{1G,B}, g_{2G,B}$	−0.0413 1.2006	0.0501 3.8667
$L_{corrG,B}$	1.7072	1.7072
$f_1 \Delta M_A + f_2$	0.0443 2.2591	
$[p_{B,min}, p_{B,max}]$	[0.1 ; 0.9]	

3.8 GHz/ Residential/ 60°		
Information	Antenna gain < 5 dBi / Measurements performed with an helicopter in and around a typical medium-sized city in France	
Parameter	**GOOD**	**BAD**
$\mu_{G,B}, \sigma_{G,B}$	3.4044 1.3980	2.5534 1.7143
$dur_{minG,B}$	10.4862	4.7289
$\mu_{M_A GB}, \sigma_{M_A GB}$	0.4640 0.7060	−2.3787 0.8123
$h_{1G,B}, h_{2G,B}$	0.3710 −19.6032	−2.3834 −24.6987
$g_{1G,B}, g_{2G,B}$	0.0332 0.5053	0.0172 0.7237
$L_{corrG,B}$	1.8017	1.8017
$f_1 \Delta M_A + f_2$	3.1149 3.5721	
$[p_{B,min}, p_{B,max}]$	[0.1 ; 0.9]	

3.8 GHz/ Residential/ 70°		
Information	Antenna gain < 5 dBi / Measurements performed with an helicopter in and around a typical medium-sized city in France	
Parameter	**GOOD**	**BAD**
$\mu_{G,B}, \sigma_{G,B}$	2.9223 1.0267	2.5188 1.3166
$dur_{minG,B}$	7.3764	7.2801
$\mu_{M_A GB}, \sigma_{M_A GB}$	−0.1628 0.5104	−2.3703 1.5998
$h_{1G,B}, h_{2G,B}$	0.1590 −20.4767	−1.0228 −22.4769
$g_{1G,B}, g_{2G,B}$	0.1137 0.4579	−0.0986 0.2879
$L_{corrG,B}$	1.3531	1.3531
$f_1 \Delta M_A + f_2$	−0.0538 5.1204	
$[p_{B,min}, p_{B,max}]$	[0.1 ; 0.9]	

4 Frequencies between 10 and 20 GHz

4.1 Rural environment

11.7 GHz/ Rural/ 34°		
Information	**Antenna gain = 19 dBi / Measurements performed with a satellite around a typical large-sized city in Germany**	
Parameter	**GOOD**	**BAD**
$\mu_{G,B}, \sigma_{G,B}$	1.7663 1.9350	−0.4722 1.7232
$dur_{minG,B}$	0.9	0.8
$\mu_{M_A GB}, \sigma_{M_A GB}$	0.05 0	−16 10.4
$h_{1G,B}, h_{2G,B}$	0 −40.25	0.87 −14.26
$g_{1G,B}, g_{2G,B}$	0 0.39	−0.21 0
$L_{corrG,B}$	0.5	0.5
$f_1\Delta M_A + f_2$	0.088 1.21	
$[p_{B,min}, p_{B,max}]$	[0.1 ; 0.9]	

4.2 Suburban environment

11.7 GHz/ Suburban/ 34°		
Information	**Antenna gain = 19 dBi / Measurements performed with a satellite around a typical large-sized city in Germany**	
Parameter	**GOOD**	**BAD**
$\mu_{G,B}, \sigma_{G,B}$	1.0125 1.6944	−0.8026 1.288
$dur_{minG,B}$	1.5	1.1
$\mu_{M_A GB}, \sigma_{M_A GB}$	−0.02 0	−5.4 7.3
$h_{1G,B}, h_{2G,B}$	0 −38.17	0.69 −15.97
$g_{1G,B}, g_{2G,B}$	0 0.39	−0.21 0
$L_{corrG,B}$	0.5	0.5
$f_1\Delta M_A + f_2$	0.036 0.80	
$[p_{B,min}, p_{B,max}]$	[0.1 ; 0.6]	